INDUCTANCE MODELING USING
NEW ELECTROMAGNETISM

by

Robert J Distinti

A thesis submitted in partial fulfillment of
the requirements for the degree of

Masters of ECE

Fairfield University

2007

Thesis advisors:

Dr. Jerry Sergent   Dr. Douglas A. Lyon

_____   _____

ABSTRACT

INDUCTANCE MODELING USING

NEW ELECTROMAGNETISM

By Robert J. Distinti

Improved electromagnetic field models, known as New Electromagnetism (NE) [NE_INTRO], are applied to model the inductance of printed and integrated circuit traces.

A review of Classical Electromagnetic theory (CE) shows many attempts to quantitatively derive a model for circuit inductance. This thesis shows that these derivations are either singular or incorrect applications of CE.

The Partial Inductance model (PI) is the current industry standard for modeling inductance [Ruehli]. The PI model is both singular and contradicts CE in at least two ways.

This paper derives a model for circuit inductance from NE which is free of singularities; furthermore, it is simpler to apply than PI and is well suited for adaptive numerical integration techniques which return accurate inductance values with processing times that are at least an order of magnitude faster than PI.

Conductive planes (ground planes) significantly affect the inductance of a circuit trace. NE provides a simple optical method to determine the inductance of a trace suspended over a single conducting plane (single plane) and the situation where a trace is sandwiched between two conducting planes (dual plane). CE applications model the single plane as simply a return path [Holloway]. No consideration is made for eddy currents induced in the plane or for the dual plane case. Microstrip and stripline geometries do consider conducting plane effects; however, these geometries are considered waveguides since the signal travels in the dielectric medium between the strip and the ground plane [Pozar]. Waveguides are a topic of follow-on work in NE.

Table of contents

1.Motivation

As the density and frequency of modern integrated circuits and printed circuits increase, the need for accurate modeling of circuit properties becomes more important. The inductance and capacitance of an integrated circuit (IC) trace is governed by its geometry, material, parasitic effects from other traces and ground planes. Any given trace could experience an unwanted resonance or "roll-off" that, under certain conditions, could lead to an intermittent failure. Capacitive and inductive coupling between traces is another source of intermittent failure.

Accurate modeling of circuit properties, prior to fabrication, reduces the number of development "re-spins". A "re-spin" is a re-design that requires new prototypes to be produced. Reduction of the number of development "re-spins" correlates to faster time to market, lower cost and improved reliability.   Reducing "re-spins" further reduces the environmental impact and cost overhead associated with short production runs required to produce prototypes.

Eliminating the uncertainty and time associated with computer modeling of vast networks of signals allows computer tuning of individual traces; thereby eliminating the wasteful "one-size fits all," "worst-case" termination methods. Utilizing this technique, device designers can reduce the power consumption of the end product; thereby, saving energy and the environment.

.

2.Historical Review

According to CE, the inductance of a circuit trace (or wire) is the summation of the self-inductance and intrinsic-inductance (A.K.A. internal inductance). There are also "parasitic" effects from other traces and ground planes; these parasitic effects are discussed elsewhere in this paper.

Before reviewing prior art, certain terms are defined for clarity. It is very important to understand the subtle differences between the terms used by circuit designers and those who study field theory. Circuit designers only have two definitions for inductive components. The first is inductance (L) and the second is mutual-inductance (M). Referring to Figure 2-1, inductance (L) relates the back-emf in a loop to the current change through the same loop. Mutual-inductance (M) relates the emf in a loop caused by the current change in another loop.

$$L \quad \text{Math Symbol} \quad M \quad \text{Loop 2}$$

$$emf = -L\frac{di}{dt} \qquad emf_2 = -M\frac{di_1}{dt}$$
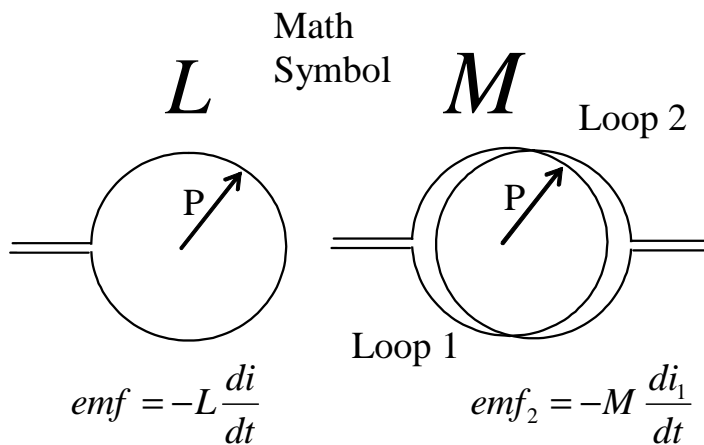
Figure 2-1: Induction terms used by circuit designers

Field theorists calculate L and M for the circuit designer based on three different field interaction models. These three field interactions are intrinsic-inductance,

self-inductance and mutual-inductance. The inductance of a circuit is the combination of self-inductance and mutual-inductance as shown by the following relationships.

L=self-inductance + intrinsic-inductance

M=mutual-inductance (same name is used for the field model)

SELF-INDUCTANCE

According to CE, the-inductance of a loop is caused by the time-rate-of-change of the magnetic flux in the space circumscribed by the loop.   The source of the magnetic field is the current in the loop. The classical field model for self-inductance is Faraday's law combined with the Biot-Savart model (all discussed later).

INTRINSIC-INDUCTANCE

The other component of inductance is known as intrinsic-inductance. This inductance is cause by the field energy inside the wire. It is developed using conservation of energy techniques, ostensibly because Faraday's law can not explain it [Hayt].

MUTUAL-INDUCTANCE

Mutual-inductance occurs when the changing magnetic field of one loop couples to a second loop. This thesis does not discuss mutual-inductance in great detail, it is proper to note that all of the classical models provide excellent results when applied to mutual-inductance problems.

Now that necessary definitions have been covered, the discussion continues with the review of prior-art.

2.1. *Faraday's law*

The most basic self-inductance problem is the single turn inductor as shown in Figure 2-2. According to CE, the self-inductance of this loop is determined from Faraday's Law (2-1), and the Biot-Savart flux model (2-3) [see Hayt].
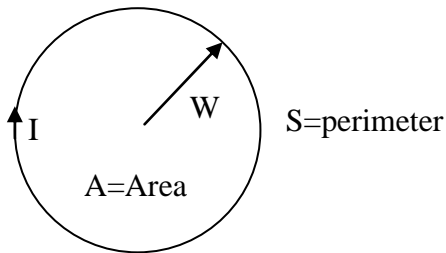

Figure 2-2

2-1) $emf = -n\dfrac{d\phi}{dt}$

2-2) $emf = -L\dfrac{dI}{dt}$

2-3) $d\mathbf{B} = K_M \dfrac{Id\mathbf{S} \times \hat{\mathbf{r}}}{|\mathbf{r}|^2}$

In the above equations, ϕ is the number of flux lines contained in (or linked by) the loop; n is the number of turns in the loop; *emf* is the voltage induced in the loop as a function of flux change; I is the current in the loop. L is the inductance of the loop; K_M is $\dfrac{\mu}{4\pi}$; B is the flux density (Webbers per square meter); r is the distance from a differential segment of wire to the point where the flux density is being determined.

First, integrate (2-3) around the perimeters to compute the flux intensity to yield

2-4) $\mathbf{B} = K_M \displaystyle\oint_S \dfrac{I d\mathbf{S} \times \hat{\mathbf{r}}}{|\mathbf{r}|^2}.$

Then substitute (2-2) into (2-1) and reduce. Allow n=1 since we are only considering single turn loops. The result is

2-5) $L = \dfrac{\phi}{I}.$

To find ϕ, we integrate (2-4) over the area circumscribed by the loop to arrive at

2-6) $\phi(I) = \displaystyle\int_A \mathbf{B} \bullet d\mathbf{A} = K_M \int_A \oint_S \left(\dfrac{I d\mathbf{S} \times \hat{\mathbf{r}}}{|\mathbf{r}|^2} \right) \bullet d\mathbf{A}.$

This resolves to

2-7) $\phi(I) = \infty$ **thus** $L = \infty$

The above results are obviously useless; a typical reaction to this result is to assume that the modeling of an inductor as a filament is the reason why the inductance goes to infinity. This is wrong for two reasons. First, the diameter of the filament is not parameterized; as such, there is no opportunity to "divide by a zero diameter". Second, this filamentary technique gives very accurate answers for mutual-inductance problems.

This model works well for mutual-inductance because the distance (r) from the primary to the area circumscribed by the secondary does not go to zero. In the self-inductance case, the primary and the second are the same; therefore, r goes to zero causing the division-by-zero event.

2.2.   *The Neumann Equation*

Another variation of Faraday's Law is called the Neumann equation (2-8) [Lorraine, Ruehli] which is derived from Faraday's Law using Vector Magnetic Potentials.

2-8) $$M = K_M \oint_S \oint_P \frac{\mathbf{dP} \bullet \mathbf{dS}}{|\mathbf{r}|}$$

The Neumann equation is expressed in terms of the mutual-inductive coupling between a primary and secondary loop as shown in Figure 2-3.
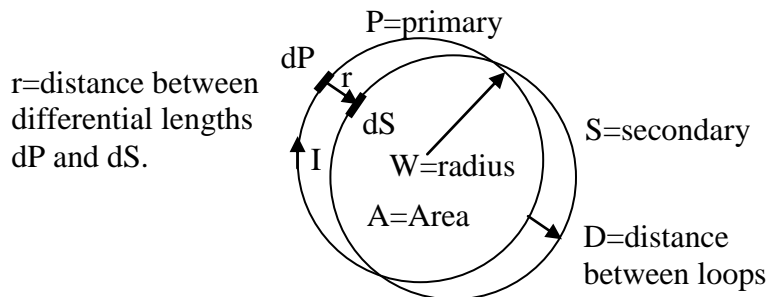

Figure 2-3 Parallel Loops

The Neumann equation (like Faraday's Law) yields an undefined answer when applied to self-inductance modeling (P and S same loop). This is obvious since r would go to zero if d goes to zero.

2.3.   *Partial Inductance (PI)*

Partial Inductance (PI) is the most successful classical attempt to address the issue of modeling circuit inductance [Ruehli]. As the name suggests, PI requires that a conductive loop be partitioned into straight sections as shown in the following diagram:

A Rectangular Loop   "Inductive Partitions"
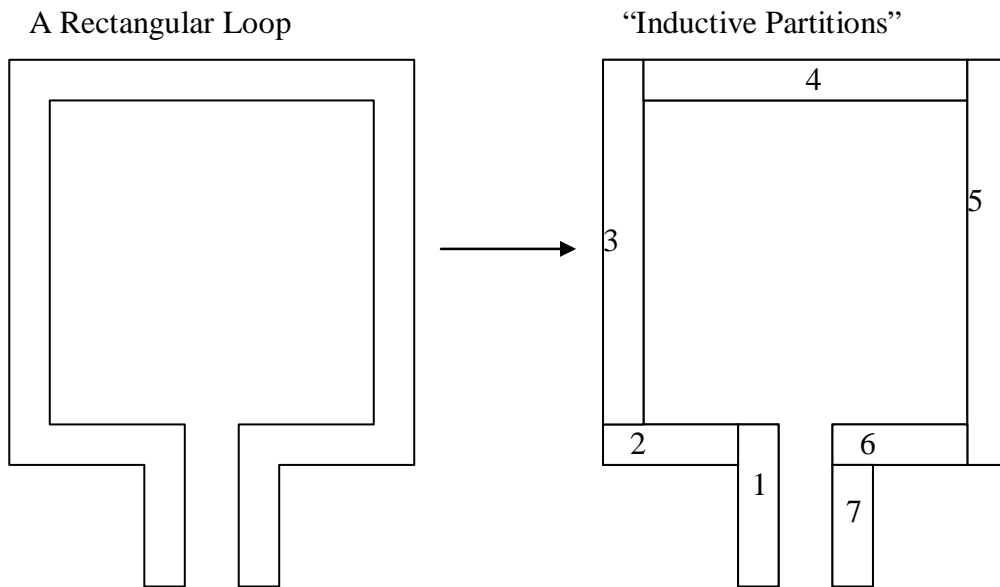
Figure 2-4: Partitioning a Loop for Partial Inductance

Once the loop is "partitioned," an "Induction matrix" is created which catalogs the "Partial Inductance" coupling between each pair of segments.

$$L_P = \begin{bmatrix} L_{p11} & L_{p12} & L_{p13} & L_{p14} & L_{p15} & L_{p16} & L_{p17} \\ L_{p21} & L_{p22} & L_{p23} & L_{p24} & L_{p25} & L_{p26} & L_{p27} \\ L_{p31} & L_{p32} & L_{p33} & L_{p34} & L_{p35} & L_{p36} & L_{p37} \\ L_{p41} & L_{p42} & L_{p43} & L_{p44} & L_{p45} & L_{p46} & L_{p47} \\ L_{p51} & L_{p52} & L_{p53} & L_{p54} & L_{p55} & L_{p56} & L_{p57} \\ L_{p61} & L_{p62} & L_{p63} & L_{p64} & L_{p65} & L_{p66} & L_{p67} \\ L_{p71} & L_{p72} & L_{p73} & L_{p74} & L_{p75} & L_{p76} & L_{p77} \end{bmatrix}$$

Each entry on the diagonal of the above matrix represents the self-inductance of a given partition (the coupling of a partition to itself) where-as the off diagonal elements represent the mutual coupling between separate partitions. Thankfully, because of reciprocity, only half the mutual terms need to be computed ($L_{Pij} = L_{Pji}$). The entries in the matrix are computed using the following Partial-Inductance equation [Ruehli]:

$$2\text{-}9)\quad L_{Pkm} = K_M \, \frac{1}{a_K a_M} \int\limits_{a_K}\int\limits_{a_M}\int\limits_{b_K}^{c_K}\int\limits_{b_M}^{c_M} \frac{\left| dl_K \bullet dl_M \right|}{r_{KM}} \, da_K \, da_M$$

The Partial Inductance Equation

Figure 2-5 highlights the parameters of equation 2-9)
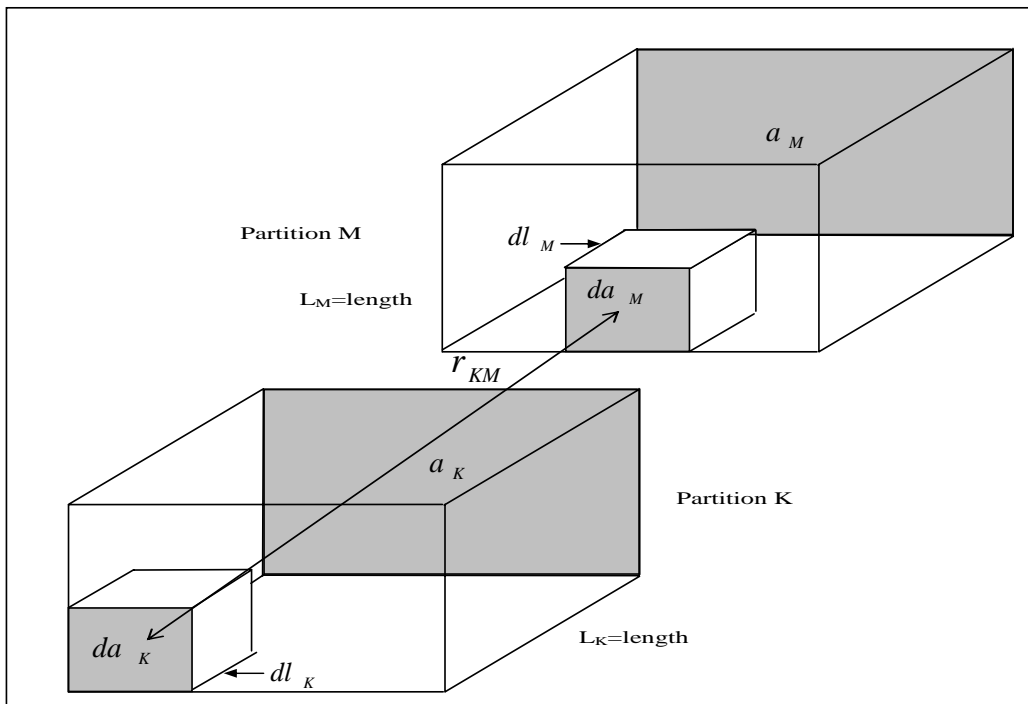
Figure 2-5:

The total inductance of the circuit is found from the matrix using the following equation:

2-10) $$L_{loop} = \sum_{K=1}^{n} \sum_{M=1}^{n} S_{KM} L_{P_{KM}}$$

Where S_{KM} is a sign function (+/-1) which takes care of the sign of the coupling between the sections.

The PI equation (2-9) is, by definition, only applicable to straight conductor partitions; therefore, the modeling non-linear shapes, such as circles, require synthesis using a number of short partitions. This correlates to a matrix of partial products equivalent to the number of partitions squared.

Ruehli develops PI from Vector Magnetic Potentials (VMP). The use of VMP requires integration around a closed loop; this is echoed in a well respected classical text book "Engineering Electromagnetics" 4th edition, the author William Hayt states the following on page 276:

> **"[The] Equation [for Vector magnetic potentials] may be written in differential form, if we again agree not to attribute any physical significance to the [result] until the entire closed path in which the current flows is considered."**

Each term in the PI matrix is defined as the emf developed in a given partition due to the magnetic field caused by the current change in another partition. By definition, this would be the inductive coupling between two linear partitions. These terms are not calculated with a closed-path integral; therefore, we can not assume "any physical significance" to their meaning. This makes sense from a classical standpoint since you need to know the magnetic flux enclosed by a

conductor in order to determine a valid emf. Since a linear partition can not enclose anything, the values obtained for the matrix are meaningless as proposed by Hayt. Ruehli tries to explain this by saying that the loops close at infinity; however, that would require integration to infinity and back in order to close the loop integral. This is certainly not shown in the equations; therefore, PI is inconsistent with CE.

Another small problem with the PI is the handling of the current at the corners of rectangular loops. Because PI only models linear partitions, the current at the corner of a rectangular loop is modeled as if it continues on in a straight path, without making the turn around the corner. A more accurate model should account for the current at the corners making a turn.

The PI model also omits the intrinsic-inductance from the result. According to classical theory, circuit inductance is the combination of the self-inductance and the intrinsic-inductance. One may argue that PI actually considers the intrinsic-inductance due to the fact that it integrates across the volume of the inductor. This would be a valid argument except for the fact that another volumetric solution (shown in the next section) involving Vector Magnetic Potentials includes intrinsic-inductance as part of the solution.

 Finally, PI exhibits the same Division-by-Zero (Singularity) problem that plagues all solutions trying to use CE. Ruehli, to his benefit, acknowledges the singularity problem (division by zero) with the diagonal elements in the matrix. He also presents a reasonable means to "Normalize" the diagonal elements.   Models where the denominator tends to zero are inherently unstable.

With the New Electromagnetism approach, there are no messy matrices, there are no "singularity" problems, there are no extraneous "sign" functions, the corners of

rectangular loops are properly modeled and finally, circular loops do not present an explosion in complexity. Before we look at NE we must complete the review of classical theory.

2.4.   Another Valiant Attempt using Classical Theory

Another valiant application of classical theory attempts to use vector magnetic potentials. This attempt is found in the text book Classical Electrodynamics by John David Jackson [Jackson]. The derivation starts on page 181 and yields the following closed form solutions (equations 2-11, 2-12) for the inductance of a loop of dimension shown in Figure 2-6.
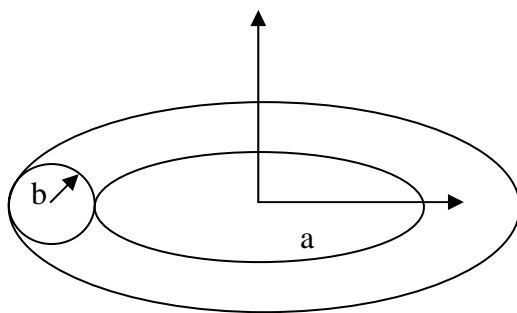
2-11) $L_{SELF} = \mu_0 a \left[\ln\left(\frac{8a}{b}\right) - 2 \right]$

2-12) $L = \mu_0 a \left[\ln\left(\frac{8a}{b}\right) - \frac{7}{4} \right]$

Figure 2-6

Jackson first derives the expression for the self-induction of the loop (2-11) before adding in the effects of intrinsic inductance to arrive at the complete answer which is equation 2-12. With careful analysis of Jackson's derivation of 2-11, it is shown that this equation is not the self-inductance of a loop; rather, it is the mutual inductance between two loops as shown in Figure 2-7 [ind_jackson].
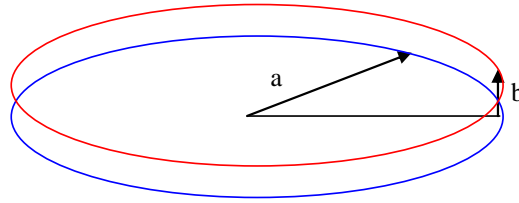
Figure 2-7

As a secondary confirmation, the Mutual-Inductance between the two loops in Figure 2-7 is derived by Maxwell using the same techniques. Maxwell's answer is:

2-13) $M = \mu_0 a \left[\ln\left(\frac{8a}{b}\right) - 2 \right]$ **[Maxwell].**

The slight difference between equation 2-13 and Jackson's result (

2-12) is due to the fact that Jackson accounts for the intrinsic-inductance. To demonstrate this, we compute the value for the intrinsic-inductance of a single loop and add it to 2-13 to arrive at the same result.

The accepted model for intrinsic-inductance is

2-14) $\frac{\mu}{8\pi}$ **(H/m)   [Hayt].**

Since the length of the loop is $2\pi a$, we get a total intrinsic-inductance component of

2-15) $\frac{\mu a}{4}$ **Henries.**

When this result is added to 2-13, we get the same answer as Jackson which is:

2-16) $\mu_0 a \left[\ln\left(\frac{8a}{b}\right) - \frac{7}{4} \right]$.

In this section it is shown that Jackson's model for a loop inductor is actually the summation of the mutual-inductance between a pair of loops and the intrinsic-induction of a single loop. This is not a valid solution for the inductance of a loop.

2.5.   Alarm Bells

Equation

2-12 is derived from Vector Magnetic Potentials and Green's theorem to allegedly compute the self-inductance of a loop. Vector Magnetic Potential is just an abstraction of the Biot-Savart model, and Greens Theorem is simply a method whereby the total flux linked by a closed loop can be found from a Vector Magnetic Potential. Therefore, these techniques are mathematically identical to using the Biot-Savart model and Faraday's law to find self-induction.

If it is not possible to develop a sensible (non-undefined) answer to self-induction from the basic models (Faraday's Law, Biot-Savart), then it can not be possible to develop a sensible answer from any abstraction of those basic models. A solution that is only possible from abstracted techniques should have set off alarm bells years ago; but it didn't. Why not? Alarm bells would certainly ring if one were to state that a certain electrostatic problem is only solvable using electric potentials and not Coulomb's Law. This is because electric potentials are derived from Coulomb's law and are thus limited to what Coulomb's law can solve; likewise, the Vector Magnetic Potential techniques for induction are derived from

the basic models (Biot-Savart, Faraday) and therefore should not be able to solve anything more than the basic models.

2.6.   *Intrinsic inductance*

As stated in the beginning of this chapter, intrinsic-inductance is the inductance of the loop due to the field energy in the wire.

Ironically, there is no classical force model that allows us to calculate intrinsic-inductance directly (this also should have set off alarm bells). Instead, a "back-door" conservation of energy approach results in $\dfrac{\mu}{8\pi}$ Henries per meter for cylindrical wire. This relation states that the intrinsic inductance is related to the length of the loop and NOT the thickness of the wire.

It would be nice to have an experiment to either confirm or deny the validity of the intrinsic-inductance component; however, this would require a stable, well-posed model of self-inductance; for which CE has yet to provide.

A simple validation experiment would measure a bunch of different length loops of different wire thicknesses. Then a "meaningful" self-inductance model would be used to subtract the self-inductance component from the measurements. If the remainder correlates to wire length and not to thickness, then we could be confident of the intrinsic-inductance effect; however, there is no meaningful self-induction model.

There is the Partial-Inductance model which seems to yield reasonable results; however, it does not consider intrinsic-inductance as part of the solution. This clearly shows a lack of consistency among classical models.

2.7.   The closed-path fallacy

Classical models do not work for self-inductance problems for a number of reasons. One reason is that electromagnetic theory is plagued by a false notion that a closed-path is required to calculate inductance. This is echoed by Weber's Caveat: "It is important to observe that the inductance of a piece of wire not forming a closed loop has no meaning" [Weber].

A simple review of dipole antenna theory shows that a dipole antenna resonates. For dipole resonance to occur; capacitance and inductance are both required; therefore, the inductance of a piece of wire not forming a closed loop has to exist.

There are many other examples that suggest the existence of straight wire inductance.

The existence of straight wire inductance implies the existence of a point-charge (or discrete) model for inductance. This is the foundation of the New Induction model which is part of New Electromagnetism.

2.8.   The Continuous Current distribution

A more significant dilemma is that classical models are hold-over's from the 1800's when current was considered "fluid like", and continuous. Since the discovery of the electron in the Early 1900's, we have come to know current to be corpuscular (or discrete) in nature; however, the old "continuous current" models are still considered valid under all conditions.

When considering a mutual-induction experiment, the distance between the two loops (primary and secondary) is substantially larger than the distance between mobile carriers (the discrete charges of interest); therefore, modeling the current in the primary as a continuous current yields a good result.

On the other hand, when considering a self-inductance experiment, we can imagine it as a mutual-induction experiment where the primary and secondary are the same loop. In that case, the distance between the primary and secondary is zero. This is the source of the singularity problem.

Ultimately what is needed is a point-charge (or discrete) form of induction allowing us to determine the induction of a wire construct at the level of the mobile carriers. New Induction provides such a model and is discussed later.

2.9.   Wrap up of Historical Review

Although Faraday's law is used to explain the mechanism of self-induction in terms of classical field theory; it provides an undefined answer when one attempts to quantitatively derive a solution for self-inductance.

The Partial Inductance model provides limited success to the self-inductance problem; however, this success comes at the price of violating classical theory. Furthermore, Partial Inductance does not properly address ground plane effects; as such, solutions to realistic PCB and IC trace inductances remain unanswered.

3.New Electromagnetism

The New Electromagnetism models were developed under the premise that ALL electromagnetic fields are generated by forcing charges to behave a certain way and ALL electromagnetic fields are measured by observing the behavior of charges; therefore, charges are the fundamental building blocks of electromagnetic physics.

Since RLC circuits are modeled with second order differential equations, there must be second order equations for electromagnetic fields. Secondly, since charges are the most fundamental building block of electromagnetism (at the electrical engineers level at least), then there must exist second order force equations based on discrete charges. That is, there must be fundamental force equations which relate charge position, velocity and acceleration.

New Electromagnetism is the expression of such force equations.

Table 3-1: The New Electromagnetism Equations

The Force Equations	Name
$\mathbf{F} = \dfrac{K_E Q_S Q_T \hat{\mathbf{r}}}{\lvert \mathbf{r} \rvert^2}$	Coulomb's Model (newtons)
$\mathbf{F} = \dfrac{K_M Q_S Q_T}{\lvert \mathbf{r} \rvert^2}\left[(\mathbf{v}_T \bullet \hat{\mathbf{r}})\mathbf{v}_S - (\mathbf{v}_S \bullet \hat{\mathbf{r}})\mathbf{v}_S - (\mathbf{v}_S \bullet \mathbf{v}_T)\hat{\mathbf{r}}\right]$	New Magnetism Model (newtons)
$\mathbf{F} = \dfrac{-K_M Q_S Q_T \mathbf{a}_S}{\lvert \mathbf{r} \rvert}$	New Induction Model (newtons)

Where: $K_M = \dfrac{\mu}{4\pi}$, $K_E = \dfrac{1}{4\pi\varepsilon}$. **Bold** letters represent vector quantities.

These equations represent the Force affecting a "target" charge due to the behavior and position of a "source" charge. The 'S' and 'T' subscripts in the

above equations delineate properties associated with the source and target charges. The vector **r** represents the vector from source to target in all equations.

Q_S

$\mathbf{a}_S$ $\mathbf{v}_S$ **r**   **F**

$\mathbf{v}_T$

Q_T
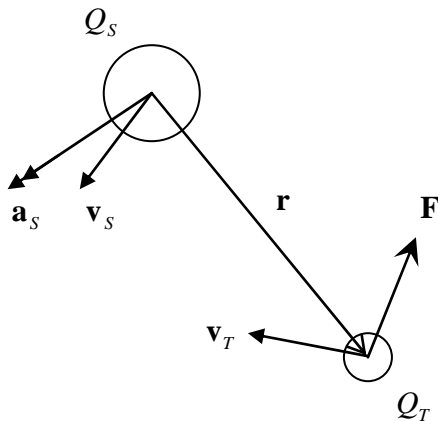
Figure 3-1: Two Body Diagram

Coulomb's model relates force to charge position. Other than notational differences, it is identical to CE.

The New Magnetism model relates force to charge velocities. The first and third terms inside the brackets can be derived directly from $F = QvxB$ and the Biot-Savart model. The middle term is required to make the model match well known experiments [Secrets]. This model differs from classical theory in that it teaches us that magnetism is actually a spherical field phenomenon; not the transverse field as depicted in the Biot-Savart model (the B-field).

The third model is New Induction which was found through computer search of experimental data. New Induction shows that an accelerating source charge creates a disturbance that expands spherically from the source. This expanding disturbance imparts a force in the opposite direction on target charges that it intersects.

Both New Induction and New Magnetism are based on a spherical magnetic field model. The magnetic field of classical theory, as described by the Biot-Savart model, is a transverse (like a donut) shaped field because it does not provide for a magnetic field longitudinally to a moving charge (see Figure 3-2); therefore, New Electromagnetism is not a reformation of classical theory; it is a superset.
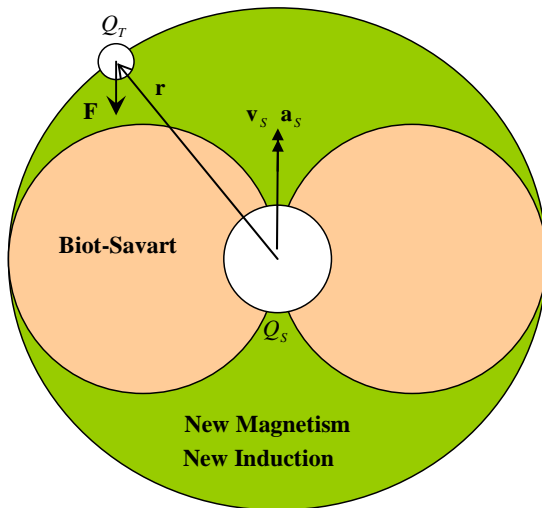
Figure 3-2 New Magnetism is a Super Set of Classical field theory

New Electromagnetism is ideally suited for modeling induction simply because the models reflect the electromagnetic interactions among discrete charges.

Lastly, the spherical field shapes are easier to model than the toroidal B-field of CE; thereby, reducing processing time and code complexity.

3.1. *New Electromagnetism Definitions*

The following definitions are required for the application of New Inductance (NI) to modeling circuit inductance.

The New Electromagnetism (NE) field models are developed by dividing the Force models by the target charge. This yields two types of force-per-coulomb fields as shown in the following table.

The Field Equations	Name
$\mathbf{E} = \dfrac{K_E Q_S \hat{\mathbf{r}}}{\lvert \mathbf{r} \rvert^2}$	Electric Field Model (Newtons/Coulomb)
$\mathbf{M} = \dfrac{K_M Q_S}{\lvert \mathbf{r} \rvert^2}\left[(\mathbf{v}_T \bullet \hat{\mathbf{r}})\mathbf{v}_S - (\mathbf{v}_S \bullet \hat{\mathbf{r}})\mathbf{v}_S - (\mathbf{v}_S \bullet \mathbf{v}_T)\hat{\mathbf{r}} \right]$	Magnetic Field Model (Newtons/Coulomb)
$\mathbf{M} = \dfrac{-K_M Q_S \mathbf{a}_S}{\lvert \mathbf{r} \rvert}$	Inductive Field Model (Newtons/Coulomb)

In CE, a force-per-coulomb field is typically designated with an "E"; however, that would imply an electric field which is conservative. In NE there are two types of force-per-coulomb fields, the Electric field (**E**) and the Magnetic Field (**M**). **E** (Electric or Electro-Potential) fields are developed from Coulomb's Model while **M** (Magnetic or Magneto-Kinetic) fields are developed from both New Induction and New Magnetism.

E fields convey potential energy and are conservative.
M fields convey kinetic energy and are not conservative.

The M field is NOT the B-field of classical theory since the M-Field truly is a "Force" field like the Coulomb field.

3.2.   Potential and Kinetic energy

New Electromagnetism provides for both potential and kinetic energy.

Potential energy (PE) is developed only from the E field and is defined by the following equation which is identical to classical theory.

3-1) $PE = -Q\int_a^b \mathbf{E} \bullet d\mathbf{L}$

This states that potential energy is acquired as a charge is moved against the applied electric field. A negative result indicates potential energy lost to other energy forms such as kinetic energy.

Kinetic energy is developed from both E and M fields. Its is defined by the following two expressions

3-2) $KE = Q\int_a^b \mathbf{E} \bullet d\mathbf{L}$

3-3) $KE = Q\int_a^b \mathbf{M} \bullet d\mathbf{L}$

These equations state that a charge acquires kinetic energy if it is allowed to move in the direction of the applied field. A negative result indicates kinetic energy lost to other forms. Other forms of energy include, but are not limited to, potential energy or energy dissipated in the form of heat.

3.3. *Potential and Kinetic voltage*

In modern text books, voltage is defined as the energy per coulomb; however, potential energy is assumed in all cases (even in the case of emf). Maxwell describes electricity in terms of kinetic and potential energies; however, the term emf is used with both in a ubiquitous manner [Maxwell].

New Electromagnetism defines two types of voltage, one for kinetic energy per coulomb (see Equation 3-4), and another for potential energy per coulomb (see Equation 3-5).

3-4) $V_K = \dfrac{KE}{Q}$ = **kinetic voltage (Joules per coulomb)**

3-5) $V_P = \dfrac{PE}{Q}$ = **potential voltage (Joules per coulomb)**

The importance of kinetic and potential voltages is discussed in the next section.

4.The Circuit Definition of Inductance

The ultimate goal of this work is to use field models to arrive at the inductance of an inductor. To this end, experiments are performed to validate the predictions of the field models; therefore, the discussion of inductance from the standpoint of circuit theory is in order.

In circuit analysis, the inductance (L) of a circuit relates the "back emf" across the inductor to the current change through it. This is shown in the following expression.

4-1) $emf = -L\dfrac{di}{dt}$ **Circuit Relationship for Inductance**

If we then solve for L, then we can determine the Inductance from measurements

4-2) $L = -emf\left/\dfrac{di}{dt}\right.$ **Induction from Circuit measurements**

The above expression enables us to determine inductance by measuring the emf across an inductor excited by a current change.

This begs the simple question: What is emf and how do we measure it?

4.1.   What is emf?

Modern texts book [Hayt] state that emf is voltage (or potential); however, this definition leads to a paradox.

The paradox is demonstrated by returning to Faraday's Law which states that a loop of wire exposed to changing magnetic field produces an emf.

4-3) $emf = -n\dfrac{d\phi}{dt}$ **Faraday's Law**

Because emf is assumed to be potential, this equation is modified using Stokes' theorem into one of Maxwell's famous equations

4-4) $\nabla \times \mathbf{E} = -\dfrac{d\mathbf{B}}{dt}$ **Maxell's version of Faraday's Law**

This equation contradicts Kirchhoff's voltage law which states that the voltage around a close loop is zero. In point form it looks as follows

4-5) $\nabla \times \mathbf{E} = 0$ **Kirchhoff's Voltage Law in point form**

Again, texts books "dance" around this issue by stating the Kirchhoff's Law is only valid for "Static" field conditions [Hayt]. This is patently ridiculous since Kirchhoff's Law is used with great success in AC circuit analysis. AC circuits are circuits where fields are certainly changing.

The proper resolution of this paradox requires us to redefine emf from magnetic sources as kinetic energy per Coulomb as opposed to potential energy per Coulomb. This notion is alluded to by Maxwell [Maxwell] in article 634 (and others) where he explicitly states that the energy in a magnetic field is kinetic in nature. By rewriting the above equation in New Electromagnetism terms we have:

4-6) $V_K = -L\dfrac{di}{dt}$ **Corrected Induction Circuit Equation**

4-7) $V_K = -n\dfrac{d\phi}{dt}$ **Corrected Faraday Law**

4-8) $\nabla \times \mathbf{M} = -\dfrac{d\mathbf{B}}{dt}$ **Corrected Maxwell Equation**

With these changes, CE induction models (4-6, 4-7, 4-8) no longer violate Kirchhoff's Law (4-5); furthermore, Kirchhoff's Law is valid under all field conditions. Finally, since the M-Field of NE is not a conservative field, then in NE, it is not a contradiction for a changing magnetic field to impart energy to a closed loop of wire.

Again, we must be able to measure kinetic voltage in order to be able to perform experimental validation of the theoretical results. All voltage measuring instruments (volt meters, oscilloscopes, etc) only measure potential voltage.

The solution to this requires us to understand what happens to a loop of wire in a changing magnetic field.

Consider a hypothetical closed loop of perfectly conducting material. Suppose the loop was exposed to a changing magnetic field characterized by a step function in such a way that kinetic energy is imparted to the loop. After the field change has settled, we are sure that kinetic energy has been imparted to the loop since we can now detect a residual magnetic field emanating from the loop due to a constant current flowing in the loop. A volt meter connected across any two points of the loop will measure nothing since Coulomb's model will ensure that the distribution of charge around the loop is uniform in spite of the fact that it is in motion.

If we were to break the loop, the kinetic energy of the current will be converted to potential energy as the moving current "crashes" into the break. This will cause charge depletion at one side of the break and charge concentration at the other side of the break leading to a Coulomb field which can then be measured by a volt meter. Because of conservation of energy, the potential voltage measured across the break will equal the kinetic voltage added to the loop by the magnetic field change.

This entire progression of events is identical to the operation of a Ballistic pendulum where the kinetic energy of a bullet is measured by capturing it in a bullet trap affixed to a pendulum. The kinetic energy of the bullet is converted to potential energy as the pendulum swings against gravity.

Therefore, the kinetic voltage developed in each inductor experiment is measured indirectly by measuring potential voltage developed across the inductor with the assumption that the conversion between potential voltage and kinetic voltage occurs fast enough to be considered instantaneous (for all practical purposes).

The exact procedures used for measuring for measuring the inductances of the experiments are discussed in the experimental section.

5.Induction using New Electromagnetism

This section details the step-by-step derivation of the inductance model for actual inductors based on the point-charge form of New Induction.

To begin this derivation we start with an assumption.

ASSUMPTION: CONSTANT CURRENT DISTRIBUTION

The following derivation assumes that the current distribution in the inductor is substantially uniform in the cross section and along the length. This assumption is common to all prior-art reviewed. A more advanced application allowing for non-uniform current distributions which is suitable for high-frequency inductors is a follow-on work.

THE SOLUTION

Solving inductance for any arbitrary conductive form is divided into two steps:

The first step is to use the New Induction model to determine the M-Field caused by a unit current change through the conductor. Only the M-Field present through the volume of the conductor is required.

The second step is to perform a volume integration of the M-Field to determine the total kinetic voltage. The total kinetic voltage per unit current change is by definition the inductance.

5.1.   *Step 1: Determining the M-Field*

The following discussion on the M-Field is applicable to conductors of all shapes and sizes. For the sake of simplicity, we consider a simple rectangular length of conductor as shown:

Current Change (dI/dt) ⟶

Current Density (J)

$$J = \frac{I}{WH}$$

$$\frac{dJ}{dt} = \frac{1}{WH}\frac{dI}{dt}$$

Height (H)

Width (W)

Length (L)
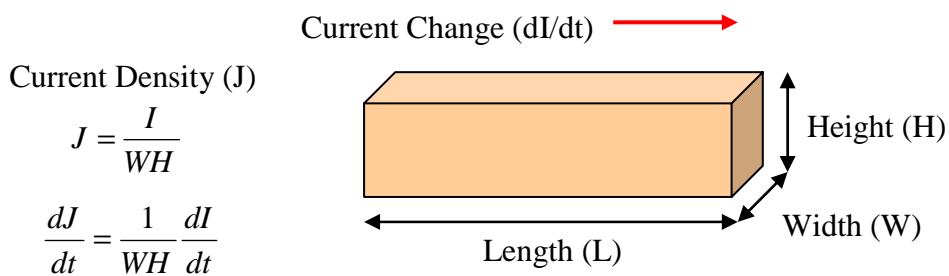
Figure 5-1: Simple conductive form

The ideal solution to mapping the M-Field over the conductor is to pick a point in the conductor; then sum the New Induction effect of all the mobile charges in the conductor to that point as shown in the following diagram.

Current change ⟶

M(x,y,z)   Mobile Carriers
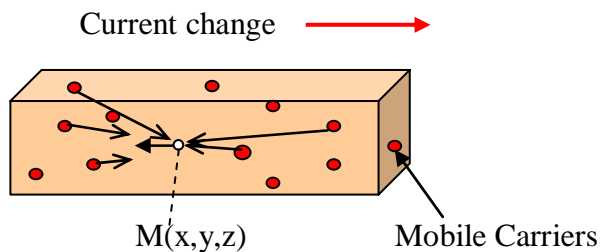
Figure 5-2: Using Discrete Model to compute the M-Field at a point inside conductor

This process is then repeated for each point where the M-Field is to be evaluated until a sufficiently dense M-Field map is generated as shown in the next diagram.

Current Change

Mobile
Carriers Not
Shown

M(x,y,z)
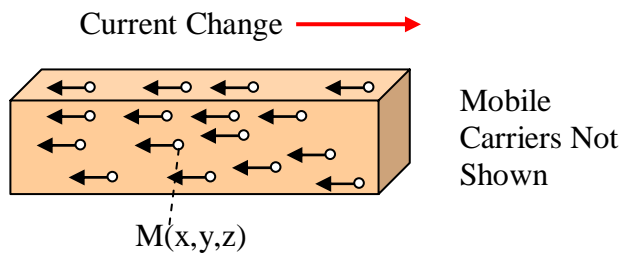
Figure 5-3: M-Field Map of conductive structure

The problem to this approach is that there are 18 coulombs of mobile carriers per cubic millimeter of copper. This would take an inordinate amount of time to compute an M-Field map.

New Electromagnetism does have continuous current models that are derived from the discrete charge models; however, we would encounter the same divide-by-zero problem that plagues CE. A practical solution is a hybrid approach.

5.1.1.   The Hybrid Approach

The hybrid approach utilizes the discrete charge models out to a certain distance from the point where the M-Field is being evaluated (called the seed). Outside of the seed, the continuous current models of New Electromagnetism are used. Therefore the M-Field at any given point is the sum of the effects of the discrete charges in the seed (the seed value) and the remainder of the conductor outside of the seed evaluated using continuous techniques.

The "Seed"

Current change

Discrete model used inside "seed" region.

Seed Size(S)

Continuous model used outside of "seed" region.

M(x,y,z)   Mobile Carriers
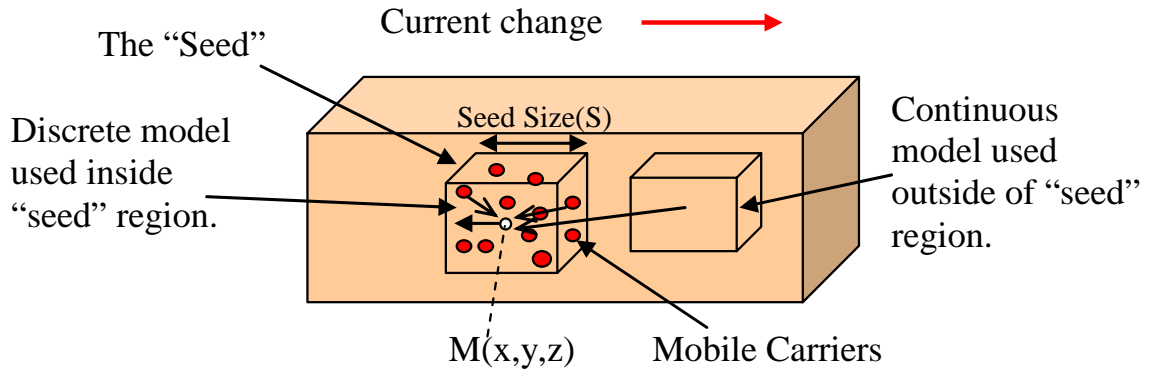
Figure 5-4: Diagram showing seed usage

5.2.   *The Seed*

The "Seed" is the region immediately around the point where the M-Field is being evaluated. Within the seed, the M-Field is evaluated using the discrete charge model of New Induction. Using this form of New Induction, the Division-By-Zero problem is avoided.

Definition: Seed Value. The seed value is the M-Field at the center of the seed due to the mobile carriers in the seed.

An advantage of this approach is that the seed value only ever needs to be computed once; this pre-computed seed value is then reused at each point where the M-Field is to be determined. For all intents and purposes it can be treated as a constant.

Care must be taken when using the pre-computed seed value since the placement can affect the answer. The following table shows the seed value contribution based on the position of the seed within the conductive material.

Table 5-1: Seed Usage

At Interior Use Whole Seed Value	At Surface Use Half Seed Value
At Edge Use Quarter Seed Value	At Corner Use 1/8 Seed Value
Other configurations where seed is partially exposed Can't use pre-computed seed value.	
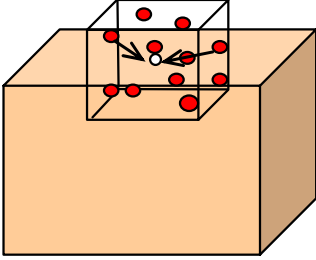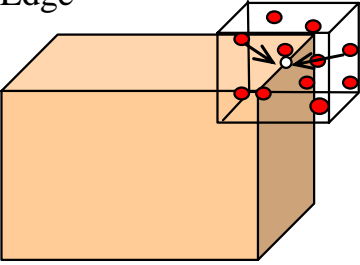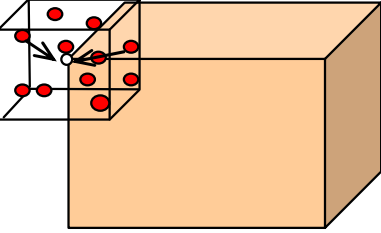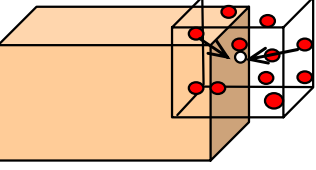
In order to use the seed value, the sample spacing of the M-Field can be no smaller that ½ the seed size (S=length of seed side). The reason for this is that when moving from an edge sample to a surface sample, the closest surface sample can be no closer than S/2 to the edge otherwise the seed will be partially exposed in such a manner that the seed value can not be used.

As a final note, it is OK to use M-Field spacing smaller than S/2 as long as any partial exposure condition where the seed value can not be used is either avoided (M-Field not considered there) or the seed contribution is computed specially for that condition.

5.2.1.   Computing the seed value for copper

Computing the seed value for a given material requires knowledge of the properties and structure of that material. Copper, along with many other conductors, have a Face Center Cubic (FCC) structure. An FCC structure is shown in the following diagram.
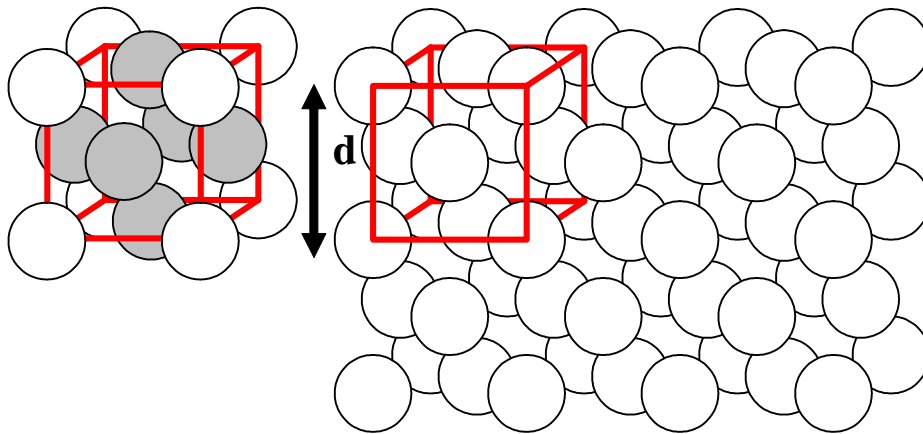

Figure 5-5: FCC structure

The FCC cell (shown by the red Cube) is aligned with its corners centered on 4 atoms. The arrangement causes atoms to be centered on each face of the cube (hence the name). This yields a total of 4 atoms per cube (6 halves at each face and 4 eighths at each corner). The size of the cell (d) is determined from the following equations [FCC].

$$d = \sqrt[3]{\frac{AtomicMass \times packing}{Avagadro \times density}}$$

Equation 5-1: Equation for length of an FCC cube

Where:
1) Packing is the number of atoms per structural cube (4 for FCC (copper))
2) Density is grams per cubic centimeter (copper=8.96 gm/cc)
3) Avogadro is Avogadro's constant = 6.022141510e23 atoms /mole
4) AtomicMass is the atomic mass (copper =63.5463 gm/mole)

Result: d=3.612e-8 cm   for copper.

Now that we have the dimension for an FCC cell, the next question is: how many FCC cells should comprise the seed? The answer is a trade-off.   Larger seed sizes allow us to reduce the M-Field integration time since more of the answer is pre-computed in the discrete part; therefore, there is less to do in the continuous part. Conversely, by increasing the seed size we reduce the resolution of the M-Field (see the final note in the previous section). There may be other factors governing selection of seed size such as the implementation of the algorithms that one chooses.

The seed size chosen for this work uses a cube of 2001 FCC cells on a side (Ns). The seed value of a cube of this size is just beyond the point where the addition of another layer of cells (2003x2003x2003) does not affect the resultant seed value by more than 0.1%. This eliminates the need to account for "half-atoms" along the face of the seed. Odd Values are chosen because it was easier to write the seed value Algorithm for an odd number of cells.

The computation of the seed value assumes that each atom in the structure contains P mobile charges that can contribute to the seed inductance. P can be a

fractional value; since, in many conductors the number of mobile carriers is not the same as the number of atoms. Furthermore, not all mobile carriers are excited when a given current is applied to the conductor; therefore, P is constrained by the applied current. This will be covered in more detail in a moment.

The M-Field value for the seed (seed value) is computed at a target atom at the center of the seed. In New Electromagnetism, a charge can not couple directly to itself; therefore, the mobile carrier around the center atom is the target which is reacting to the M-Field; therefore, it can not be a contributor.

The M-Field value is computed at the center atom using a summation of the New Induction Field model ($\mathbf{M} = \dfrac{-K_M Q_S \mathbf{a}_S}{|\mathbf{r}|}$) over the remaining atoms in the seed. This is shown in the following equation:

5-2) $\quad \mathbf{M}_{center} = -K_M \sum\limits_{n=1}^{total} \dfrac{Q_n \mathbf{a}_n}{|\mathbf{r}|} \quad \{n \neq center\}$

Since P represents the quantity of active mobile carriers per atom, Q is replaced by P. Also, since the density of current change is assumed to be uniform, then the charge acceleration ($\mathbf{a}_n$) is the same for all active mobile carriers; therefore, the equation is rewritten as follows:

5-3) $\quad \mathbf{M}_{center} = -K_M P\mathbf{a} \sum\limits_{n=1}^{total} \dfrac{1}{|\mathbf{r}|} \quad \{n \neq center\}$

We next make the following definition

5-4) $RawSeedValue = RSV = \sum\limits_{n=1}^{total} \dfrac{1}{|\mathbf{r}|}$ $\{n \neq center\}$

The RSV can be computed using a number of simple algorithms. The RSV for a Ns^3 (2001x2001x2001) cell copper seed is

1.906919e7 (atoms/length).

The seed size (Length of side) is computed by multiplying Ns times the cell size (d).

5-5) $S = dN_S$

Next we compute the value of P and the acceleration ($\mathbf{a}$). We start by considering that the seed is at the interior of a conductive form (such as a printed circuit board trace).

Assuming a conductor with a rectangular cross section (HW) the current density (J) entering the conductor is:

5-6) $J = \dfrac{I}{HW}$

The amount of current that is passing through the seed (I_S) is found by multiplying the current density (J) by the cross sectional area of the seed (S*S).

5-7) $I_S = I \dfrac{S^2}{HW}$ **(Current through seed)**

Then we use the following identity which states that the current (I) along a length of a conductor (L) is equivalent to a quantity of charge (Q) moving at velocity (v).

5-8) $I\mathbf{L} = Q\mathbf{v}$ (L **and** v **in same direction).**

Using the side of the seed that is aligned with the conductor ($S\hat{\mathbf{L}}$) for **L** and I_S for I yields the total charge motion in the seed related to the charge entering the entire wire structure

5-9) $\quad Q\mathbf{v} = I \dfrac{S^3}{HW}\hat{\mathbf{L}}$

Take the time derivative of both sides

5-10) $\quad Q\mathbf{a} = \dfrac{dI}{dt}\dfrac{S^3}{HW}\hat{\mathbf{L}}$

Q is the total charge moving in the seed. We convert Q to P by dividing by the number of atoms in the seed which is the total number of cells ($N=Ns^3=2001^3$) times the number of atoms per cell (4 for FCC), thus

5-11) $\quad P\mathbf{a} = \dfrac{1}{4N}\dfrac{dI}{dt}\dfrac{S^3}{HW}\hat{\mathbf{L}}$

 Substituting this into the equation for M yields

5-12) $\quad \mathbf{M}_{Seed} = -K_M \dfrac{1}{4N}\dfrac{dI}{dt}\dfrac{S^3}{HW}[RSV]\hat{\mathbf{L}}$ **Seed Value**

This result is set aside; the next objective is to compute the effect at the center of the seed due to the rest of the conductor (outside the seed). This is done with the continuous current form of New Induction.

5.2.2. Developing the Continuous current model

Again, we start with the New Induction field equation

5-13) $\mathbf{M} = \dfrac{-K_M Q_S \mathbf{a}_S}{|\mathbf{r}|}$

and the charge velocity identity

5-14) $I\mathbf{L} = Q\mathbf{v}$ (L is a vector length).

Take the time derivative of identity (5-14) and substitute into (5-13) to yield

5-15) $\mathbf{M} = -K_M \dfrac{dI}{dt} \dfrac{\mathbf{L}_S}{|\mathbf{r}|}$.

Then take the derivative of (5-15) with respect to length to establish the quantity of M-Field contributed by each differential length of the source ($\mathbf{L}$s). Also, drop the s subscript so as not to misidentify this as the length of seed.

5-16) $d\mathbf{M} = -K_M \dfrac{dI}{dt} \dfrac{d\mathbf{L}}{|\mathbf{r}|}$

We can consider a wire as a collection of filaments of cross section da; where the current in each filament is J*da and J is computed the same as in the seed section, thus

5-17) $d^2\mathbf{M} = -K_M \dfrac{dI}{dt} \dfrac{da}{HW} \dfrac{d\mathbf{L}}{|\mathbf{r}|}$.

To compute M, we then perform volume integration and arrive at

5-18) $\mathbf{M} = -K_M \dfrac{dI}{dt} \dfrac{1}{HW} \displaystyle\int_L \int_a \dfrac{da\, d\mathbf{L}}{|\mathbf{r}|}$.

Since this must only be performed exterior to seed, we add the following restriction:

5-19) $\mathbf{M}_{ext} = -K_M \dfrac{dI}{dt} \dfrac{1}{HW} \displaystyle\int_L \int_a \dfrac{da\, d\mathbf{L}}{|\mathbf{r}|}$ (a, L external to seed)

To reiterate: Equation 5-19 is the component of the M-Field at the center of the seed that results from current changes external to seed.

5.2.3. Mapping the M-Field

The total M-Field is computed at any given point by summing the M-Field contributed by the seed and the M-Field contributed by current changes external to the seed.

5-20) $M_{total}=M_{seed}+M_{ext}$

The following diagrams show the magnitude of the M-Field mapped over the volume of length of conductor. Figure 5-6 shows the magnitude at the surface (less the ends) and Figure 5-7 shows cuts through the volume at regular intervals. The false color rendition represents maximum magnitude with the color white and least magnitude with black (not necessarily zero).
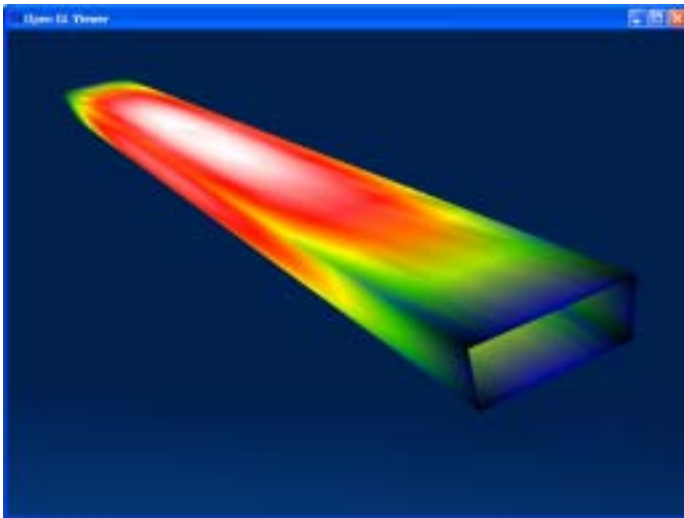

**Figure 5-6: M-Field Map of conductor surface**
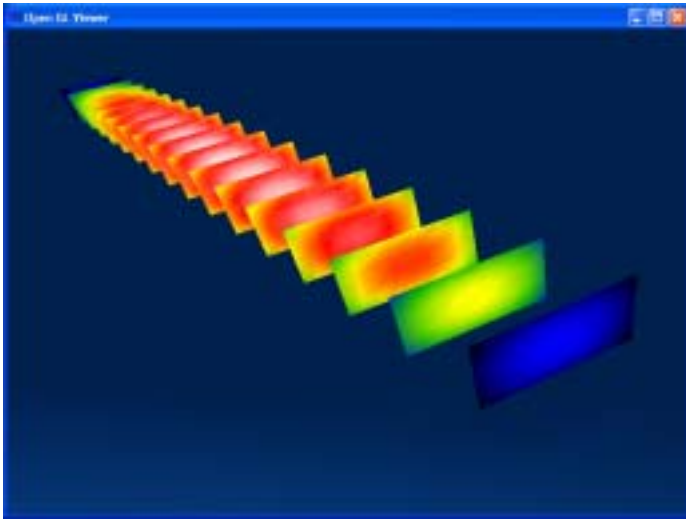
**Figure 5-7: M-Field map of cuts through conductor**
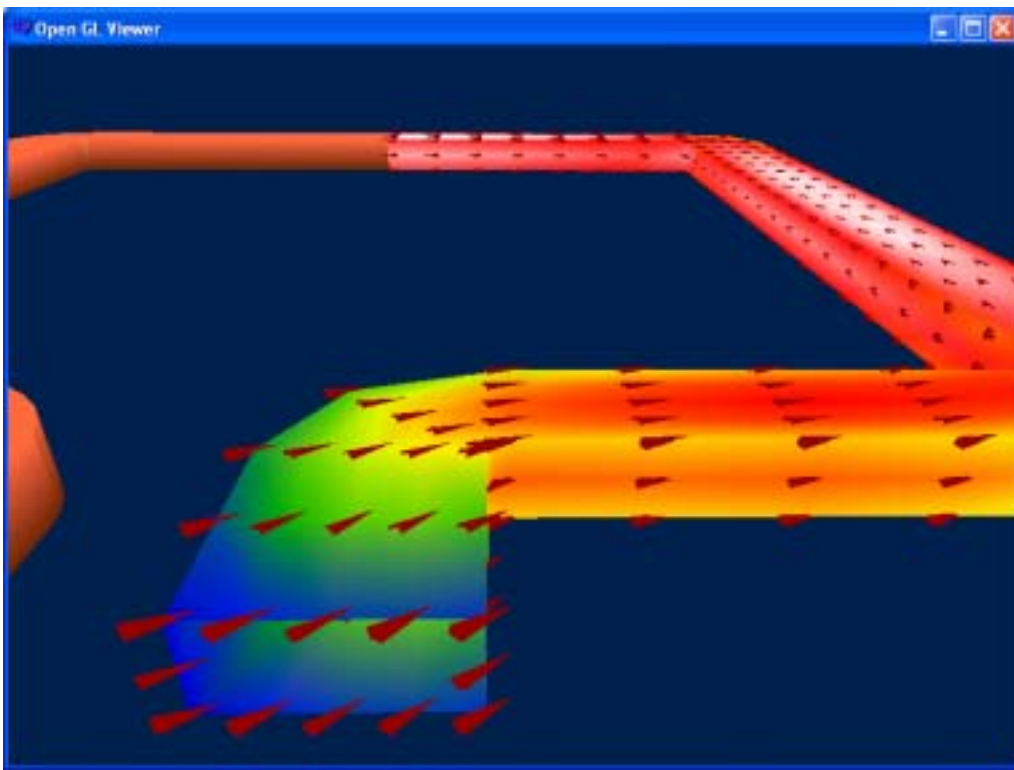
Figure 5-8: M-Field map of rectangular loop with vanes showing field direction.

5.3. The Second Step: Integrate the M-Field to find the Kinetic Voltage

Once the M-Field is known, the second step is to determine the total kinetic voltage by integrating the M-Field. If the wire structure were filamentary, then the kinetic voltage could be found with the following simple path integral:

5-21) $V_K = \int \mathbf{M} \bullet d\mathbf{L}$

Since a real inductor is not filamentary and the M-Field is neither conservative nor uniform, we must perform volume integration over the M-Field to determine the average kinetic voltage as shown in Figure 5-9 and equation 5-22.

$$V_K = \int_L \mathbf{M} \bullet d\mathbf{L}$$

dA

Current Change

$A = HW$

$$V_K = \frac{1}{A} \int_A \int_L (\mathbf{M} \bullet d\mathbf{L}) dA$$
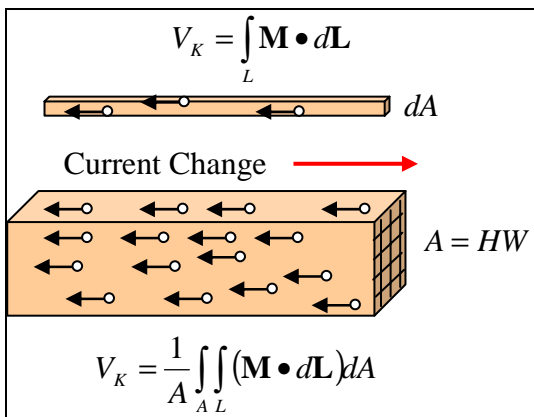
Figure 5-9: Integrals Yielding Kinetic Voltage

5-22) $V_K = \dfrac{1}{HW} \int_A \int_L (\mathbf{M} \bullet d\mathbf{L}) dA$

Remember that $L = -\dfrac{V_K}{dI/dt}$ Thus:

5-23) $L = -\dfrac{1}{HW} \dfrac{1}{dI/dt} \int_A \int_L (\mathbf{M} \bullet d\mathbf{L}) dA$ **Inductance from the M-Field**

Equation 5-23 is the final step of the hybrid method for computing the inductance of an inductor from NE. The first step is to compute the M-Field from equations 5-12, 5-19 and 5-20. The result of which is then inserted into Equation 5-23.

Note: since the M-Field determined in the first step will be a discrete set of points (a numerical process is assumed); then equation 5-23 will likewise need to be adapted for numerical methods.

6.Comparison

For the sake of comparison, allow the seed size to diminish to zero. This allows equation 5-19 to comprise the entire solution for the M-Field.

Substituting (5-19) into (5-23) and reducing yields

$$\textbf{6-1)} \quad L = K_M \frac{1}{(HW)^2} \int_A \int_{L_K} \int_{L_M} \left(\frac{d\mathbf{L}_m \bullet d\mathbf{L}_n}{r_{KM}} \right) dA$$

Unlike the Hybrid Model described in the previous section, this model will result in singularities; however, it puts us on the same footing as PI for the sake of comparison.

6.1.   Comparing to Partial Inductance

If we were to substitute the same subscript notation as Partial Inductance into equation 6-1, we arrive at:

$$\textbf{6-2)} \quad L = K_M \frac{1}{(HW)^2} \int_{a_K} \int_{a_M} \int_{L_K} \int_{L_M} \left(\frac{d\mathbf{L}_m \bullet d\mathbf{L}_n}{r_{KM}} \right) da_K \, da_M$$

Then generalize it for any arbitrary cross sectional area

$$\textbf{6-3)} \quad L = K_M \frac{1}{a_K a_M} \int_{a_K} \int_{a_M} \int_{L_K} \int_{L_M} \left(\frac{d\mathbf{L}_m \bullet d\mathbf{L}_n}{r_{KM}} \right) da_K \, da_M$$

The Continuous Current Model of New Induction

Then compare it to Partial Inductance

$$L_{Pkm} = K_M \ \frac{1}{a_K a_M} \int\limits_{a_K}\int\limits_{a_M}\int\limits_{b_K}^{c_K}\int\limits_{b_M}^{c_M} \frac{\left| dl_K \bullet dl_M \right|}{r_{KM}} da_K \, da_M$$

The Partial Inductance Model

Partial Induction may look remarkably like the New Induction results; except that the "absolute value" function around the dL's makes this model more difficult to apply. The absolute value of the dot product requires PI to include a separate sign function that would not otherwise be necessary.

The New Induction result is the model for the WHOLE inductor, regardless of shape or size; whereas the Partial Induction Model is only the solution for a linear section of the loop since PI requires a non-linear inductor to be partitioned. The following table breaks down the other comparisons.

Table 6-1: Comparison of New Induction to Partial Inductance

	New Induction	**Partial Induction**
Singular	Not if using the seed	Yes
Types of inductors handled	Applies to any shape inductor.	Only applies to linear inductors. Requires "partitioning" and matrix operations to handle inductor shapes more complicated than a straight section
Treatment of corners	Proper handling of corners	Corners are a source of error
Treatment of circles or curves	No change to basic equation	Requires a synthesis using large quantity if straight sections. Thus requiring very large matrix.

Extra requirements	The seed methodology (Chapter 5) prevents the singularity	1)A sign function that relates the sign of the partitions 2) Matrix reduction technique for complex geometries 3) A normalization scheme to handle the singularity issue
Scientific basis	The spherical field models of New Electromagnetism	Violates classical theory; closed loop requirements of VMP are dropped, requires loops to close at infinity but this is not done.
Intrinsic Inductance	Not needed, New Induction is complete.	Although Ruehli does not mention it in his paper on PI, other researchers account for it in their applications of PI or other methods [Holloway, Jackson, others].
Processing time (see later section)	Proportional to wire volume	Proportional to the square of wire volume
Single Ground Plane (see later section)	Image method. Requires integration over the wire volume a second time.	Considers the ground plane only as a current return path [Holloway]. Requires integration of a considerable volume of the ground plane.
Dual Ground Plane (see later section)	Image method. Requires integration over the wire volume many times depending upon desired accuracy.	No application found.

7.Ground Plane/Conducting Plane Effects

When multi-layer printed circuits are constructed, one or more of the layers are typically used to distribute power or ground; as such, these layers are substantially solid except for vias or perhaps a few odd traces that could not be fit in the routing planes.

In some cases, conducting planes are inserted for shielding purposes; in other cases, ground planes are required to ensure the proper impedances for stripline and microstrip circuits.

A conductive plane severely affects the inductance of a PCB trace; therefore, any practical application requires that these effects be taken into account.

For this section we use the term ground plane; however, the techniques described in this section apply to any conductive plane regardless of whether it is connected to a given potential or not.

Classical attempts to account for ground plane effects consider the ground plane only as a return path [Holloway]. There is no provision to account for the eddy currents induced in the ground plane or for the effects of a plane which is not part of the circuit. The classical approach applies PI to the return current distribution in the ground plane which leads to extensive computer processing time since a volume substantially larger than the original trace must be integrated. Furthermore, since the current distribution in the ground plane is not uniform, many partitions are required which greatly expands the size of the inductance matrix that needs to be generated and reduced.

New Electromagnetism provides a simple technique to model the effects of a conductive plane.   This technique is similar to the method of images developed for electrostatic charges [HAYT]. The difference is that the plane does not have to be tied to a potential, nor does the plane have to be part of the circuit.

We begin by considering a quantity (Q) of charge accelerating over a conductive plane (refer to Figure 7-1). We refer to this as the source charge for the sake of discussion. According to New Induction, the accelerating source charge produces an M-Field which forces the charges in the ground plane to accelerate in the opposite direction. The accelerating ground charges in turn produce their own M-Field which in turn affects the source charge.

Accelerating charge (The Source Charge)

Currents induced in ground plane from M field of accelerating charge

h=height above plane
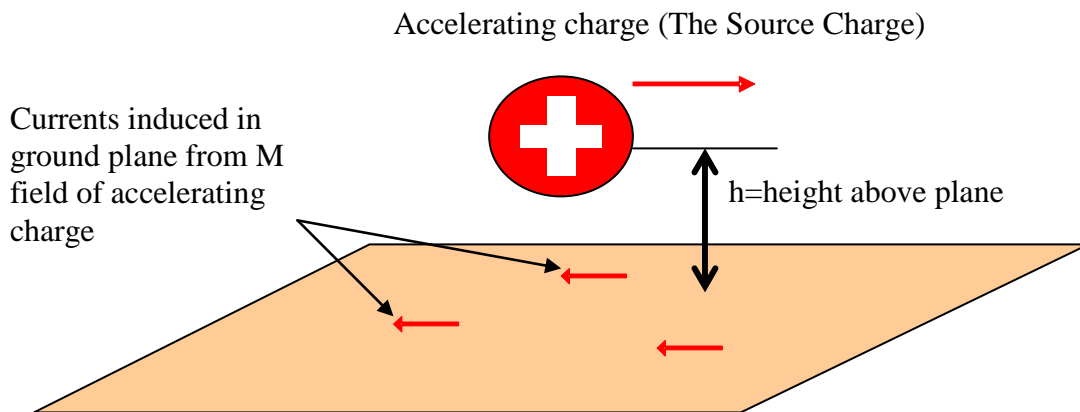
**Figure 7-1: Source Charge Accelerating Over Ground Plane**

The question is: how do the induced currents in the ground plane affect the source charge?

Through symmetry, we realize that a charge accelerating on the opposite side of the plane induces the same ground plane currents (we are using the same assumptions from the method of images of electrostatic theory [HAYT]). We shall refer to this as the Image Charge.

Currents induced in ground plane from M-Field
of "Image Charge"

-h

Charge on opposite side (Image
Charge) accelerating in same
direction as Source Charge.
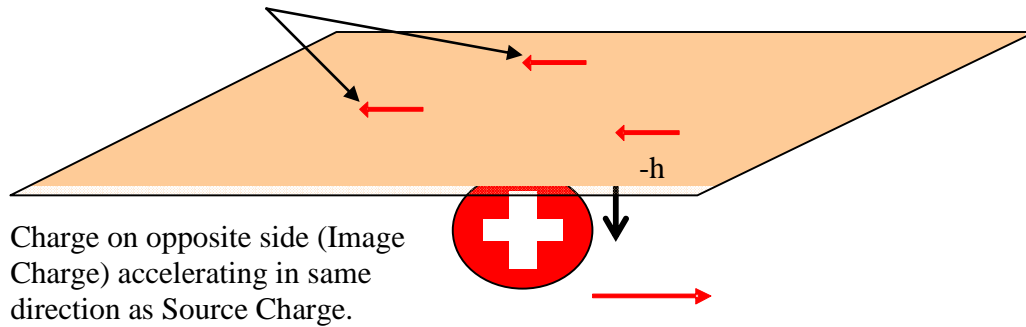
Figure 7-2: Charge on opposite side (Image Charge) produces same ground plane currents

We observe that the ground plane currents are accelerating in the opposite direction to either the source or image charge; therefore, we can remove the ground plane as long as the direction (or polarity) of the image charge is reversed.

Source Charge

Source Charge

2h

2h

OR

Negative
Direction
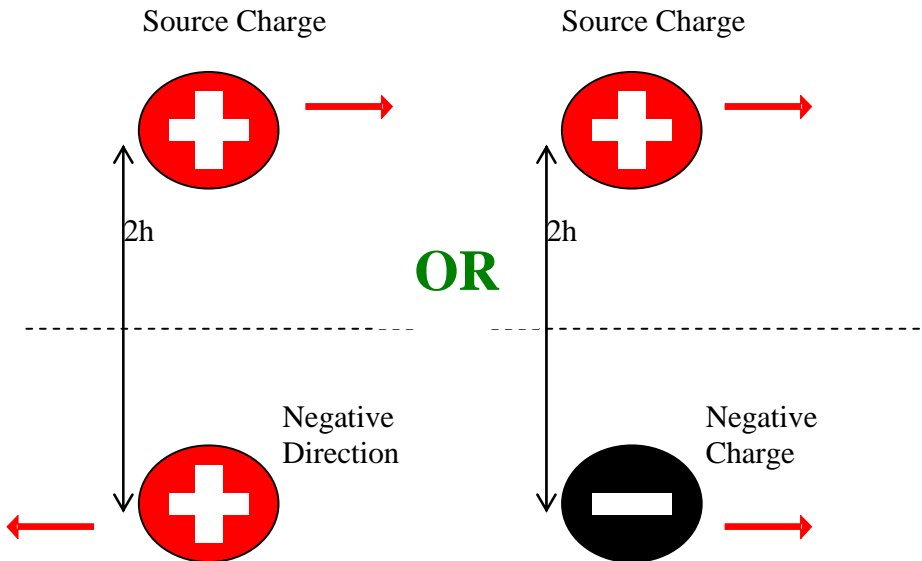
Negative
Charge

Figure 7-3: Ground plane effects Simulated with Negative Image

Thus, the NE approach to modeling the effect of a ground plane is to use the negative image of the current carrying construct.   The technique is applicable to high frequency modeling as long as propagation delays are accounted for [NIA1].

Since copper is not a perfect conductor, we can't use 100% of the image. Experiments show that a 1OZ copper plane (1.35 mils thickness) has an "inductive reflectivity" of 97% [NIA1].

The following rendering (Figure 7-4) shows the M-Field of three basic inductor shapes without considering the ground plane effects. Notice that the circle and rectangle are only half mapped, this is done to reduce processing time since, due to symmetry, the other half will be the same.
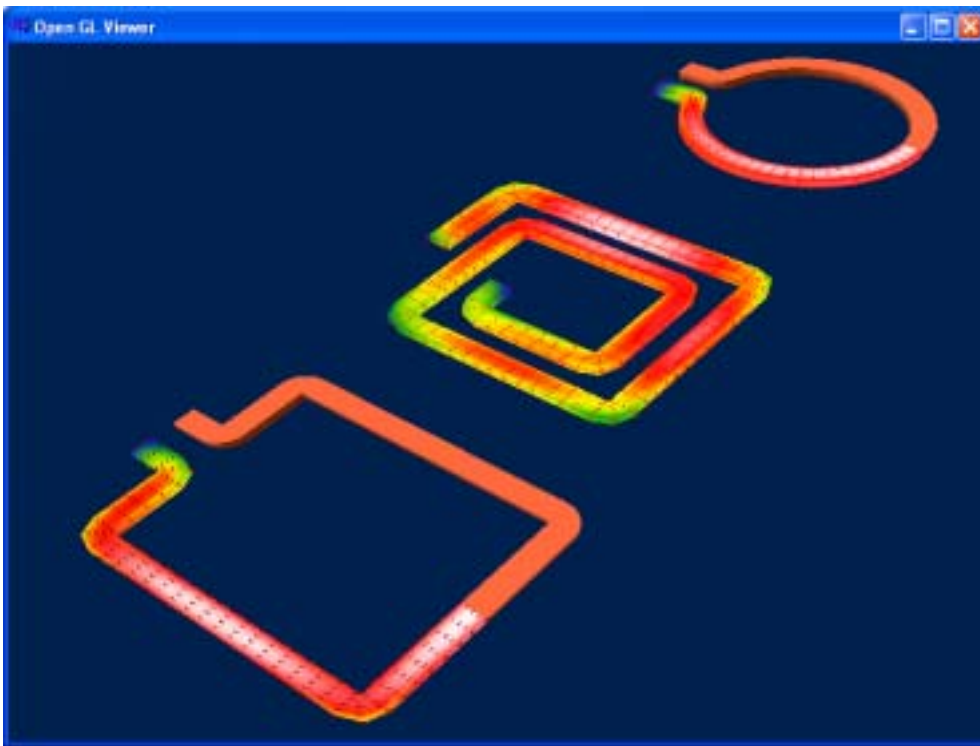

Figure 7-4: M-Fields of three basic inductor shapes

The next rendering (Figure 7-5) shows the three basic shapes again except that their negative ground plane images are enabled. Notice that the intensities of the M-Field mappings are substantially reduced.
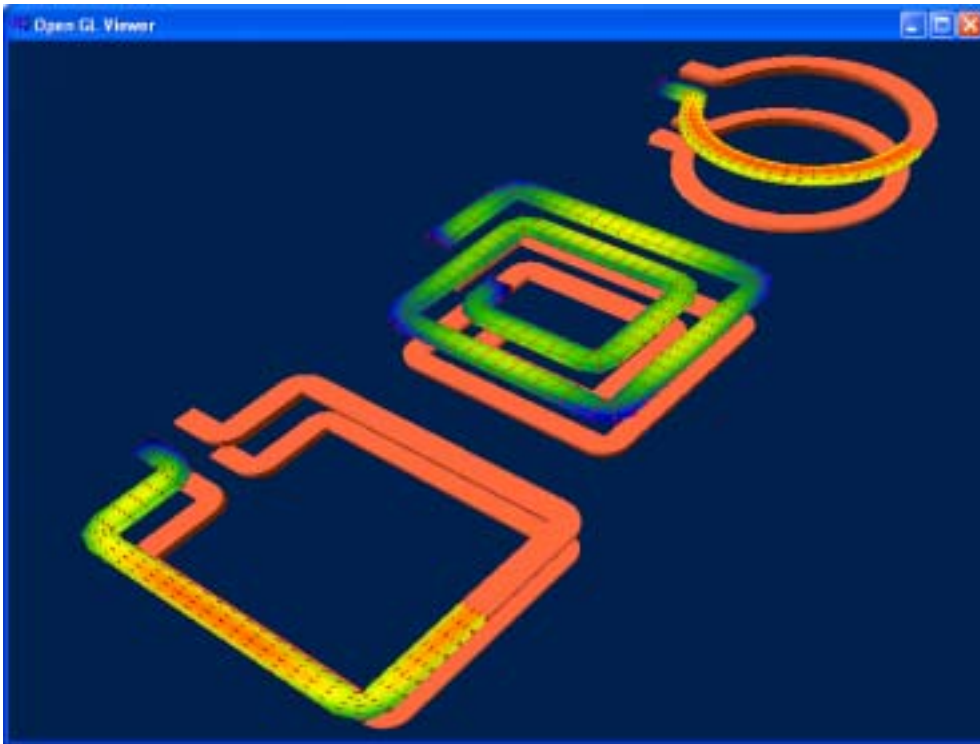
Figure 7-5: The three basic shapes with ground plane images enabled

As a final note, this technique assumes that the ground plane extends sufficiently beyond the shape and that there are no significant obstructions to current flow in the ground plane (such as cuts in the copper).

7.1.1.   Dual Conducting Planes

If a circuit trace is sandwiched between two planes, it is not enough just to have two images (one above and one below). Now the reflections of reflections must be accounted for until the inductive reflectivity (97% for copper) diminishes the effect [NIA1]. This is similar to the effect demonstrated in Figure 7-6 which shows a candle situated between two mirrors.
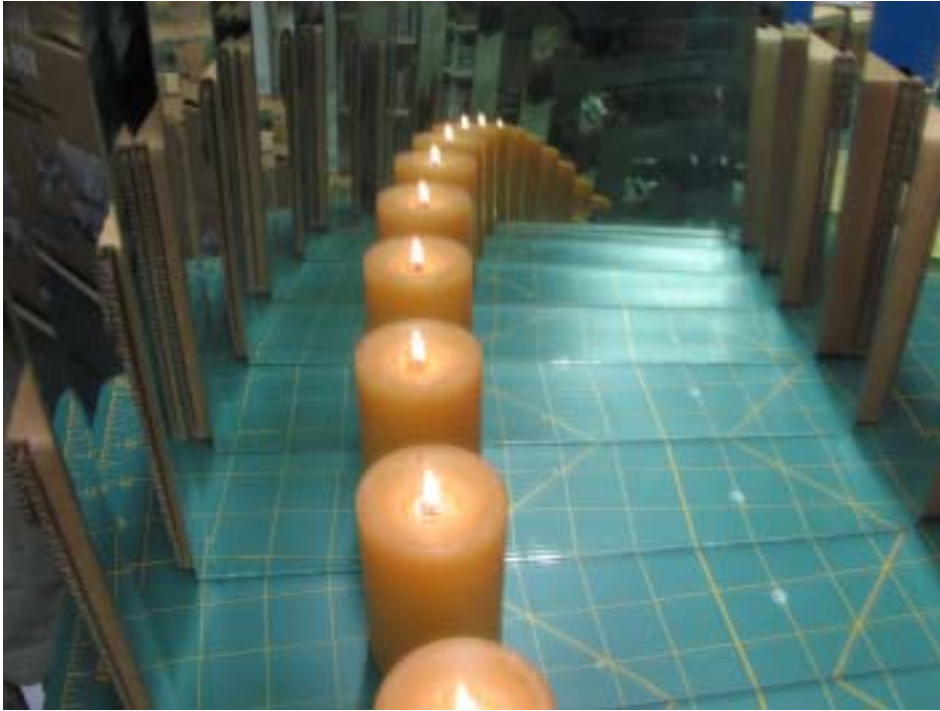
Figure 7-6: Reflections of Reflections
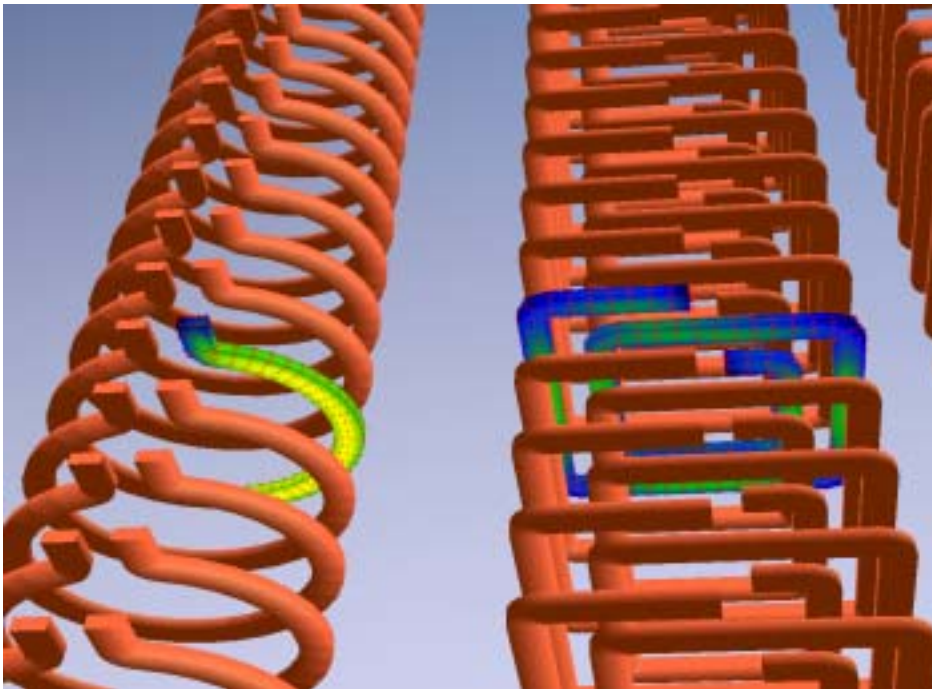
Figure 7-7: Rendering showing multiple images of circle and spiral

For the inductor case, each time the image is reflected, it is negated and its intensity reduced to 97%. This results in alternating image coefficients as shown in Figure 7-8
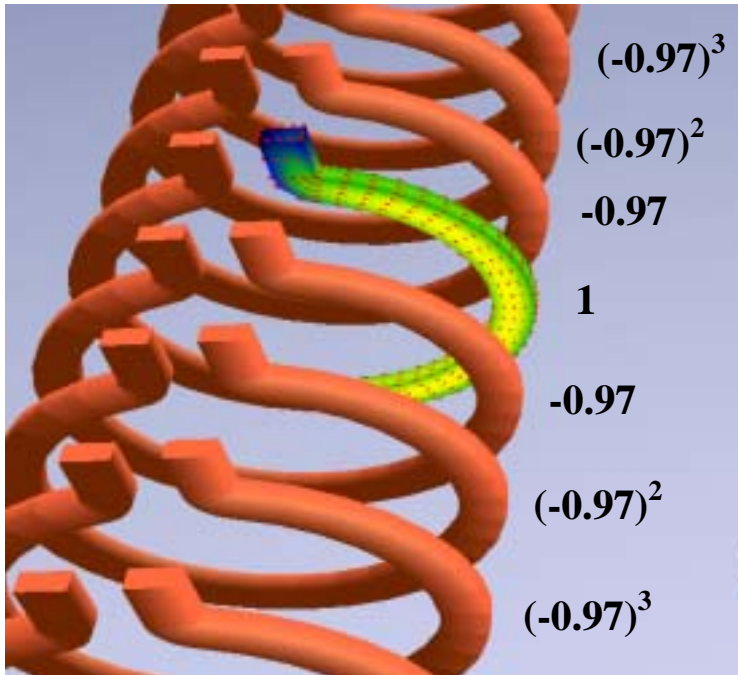
Figure 7-8: Computing the coefficients for 3 pairs of reflected images

By definition, an image pair consists of the corresponding images on either side of the original. Figure 7-9 shows how the induction algorithm converges as the number of image pairs is increased. Because of the symmetry of the convergence, it should be possible to determine the dual plane value from just a few images; however, that task will be left for follow-on work. For now, dual plane values are computed with 70 pairs of reflections.

Note: convergence will vary depending upon conducting plane material and the distance from the circuit trace to the plane.
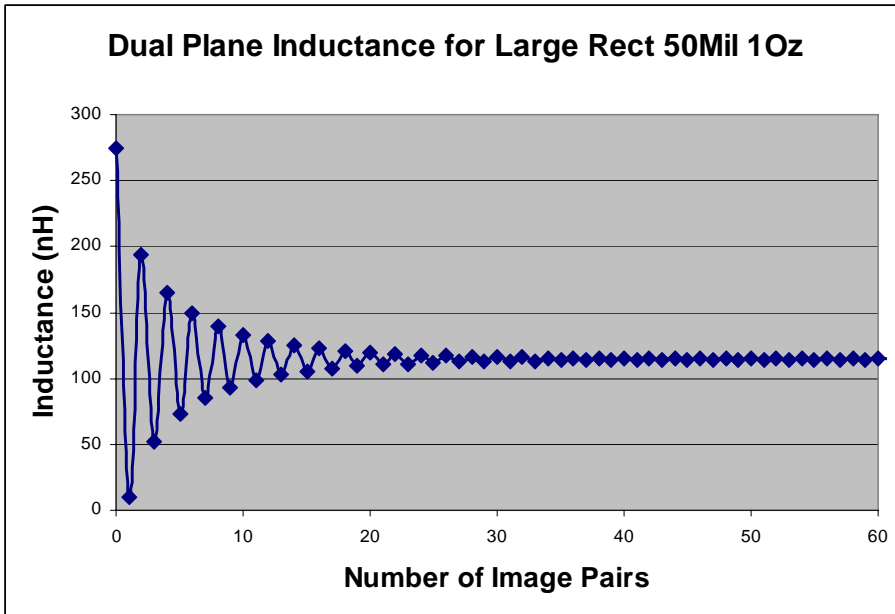
Figure 7-9: Dual Plane Convergence

8.Validation

To validate the New Induction solution, a range of various experiments involving the following shapes were chosen:

Rectangle

H=Copper Thickness

W

A

B

D

C

Circle

H=Copper Thickness

W

A

D

C

Spiral: Center-lead

B

W

A

C

C

H=Copper Thickness
N=Number of turns

Spiral: Corner-lead

B

W

A

C

C

H=Copper Thickness
N=Number of turns
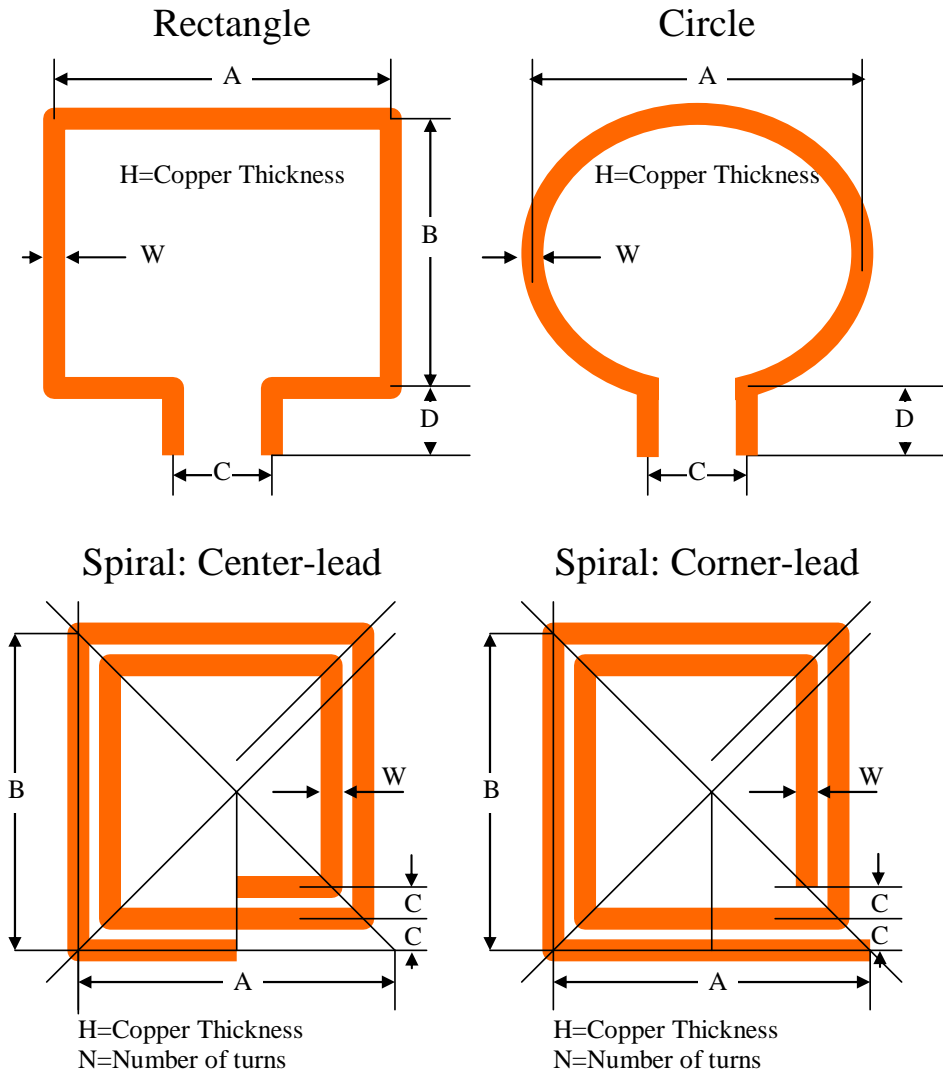
Figure 8-1: PCB inductor shapes and dimensions

The following table lists the experiments.

Experiments				Dimensions						
Exp	Thick	Shape	CP	A	B	C	D	N	H	W
n	Oz			mils	mils	mils	mils		mils	mils
1	1oz	Large Rect	No	2600	3300	600	200		1.35	50
2	1oz	Large Rect	Yes	2600	3300	600	200		1.35	50
3	1oz	Small Rect	No	2300	2450	200	400		1.35	50
4	1oz	Small Rect	Yes	2300	2450	200	400		1.35	50
5	1oz	Spiral	No	2150	2150	150	0	4	1.35	50
6	1oz	Spiral	Yes	2150	2150	150	0	4	1.35	50
7	1oz	Large Rect	No	2600	3300	600	200		1.35	30
8	1oz	Large Rect	Yes	2600	3300	600	200		1.35	30
9	1oz	Small Rect	No	2300	2450	200	400		1.35	30
10	1oz	Small Rect	Yes	2300	2450	200	400		1.35	30
11	1oz	Spiral	No	2150	2150	150	0	4	1.35	30
12	1oz	Spiral	Yes	2150	2150	150	0	4	1.35	30
13	1oz	Large Circle	No	2400		300	200		1.35	50
14	1oz	Large Circle	Yes	2400		300	200		1.35	50
15	1oz	Small Circle	No	1800		100	450		1.35	50
16	1oz	Small Circle	Yes	1800		100	450		1.35	50
17	1oz	Large Circle	No	2400		300	200		1.35	30
18	1oz	Large Circle	Yes	2400		300	200		1.35	30
19	1oz	Small Circle	No	1800		100	450		1.35	30
20	1oz	Small Circle	Yes	1800		100	450		1.35	30
21	2oz	Large Rect	No	2600	3300	600	200		2.7	50
22	2oz	Large Rect	Yes	2600	3300	600	200		2.7	50
23	2oz	Small Rect	No	2300	2450	200	400		2.7	50
24	2oz	Small Rect	Yes	2300	2450	200	400		2.7	50
25	2oz	Spiral	No	2150	2150	150	0	4	2.7	50
26	2oz	Spiral	Yes	2150	2150	150	0	4	2.7	50
27	2oz	Large Rect	No	2600	3300	600	200		2.7	30
28	2oz	Large Rect	Yes	2600	3300	600	200		2.7	30
29	2oz	Small Rect	No	2300	2450	200	400		2.7	30
30	2oz	Small Rect	Yes	2300	2450	200	400		2.7	30
31	2oz	Spiral	No	2150	2150	150	0	4	2.7	30
32	2oz	Spiral	Yes	2150	2150	150	0	4	2.7	30
33	1oz	Large Rect	Dual	2600	3300	600	200		1.35	50

Table 8-1 Experiment dimensions

Dual Plane Experiments				Dimensions						
Exp	Thick	Shape	CP	A	B	C	D	N	H	W
n	Oz			mils	mils	mils	mils		mils	mils
33	1oz	Large Rect	Dual	2600	3300	600	200		1.35	50
34	1oz	Large Rect	Dual	2600	3300	600	200		1.35	30
35	1oz	Large Circle	Dual	2400		300	200		1.35	50
36	1oz	Large Circle	Dual	2400		300	200		1.35	30

Table 8-2 Dual Plane Experiment dimensions

Note: In the above tables, blank entries represent dimensions that are not applicable to the given geometry. For example, circles do not specify a B dimension (see Figure 8-1)

The column 'CP' refers to conductive plane. Each loop is measured without conducting planes, then again with a single conductive plane. Some loops are measured with dual conducting planes as shown in Table 8-2.

Not all of the inductors are used in the dual plane measurements because the dual plane techniques were not originally planned for this thesis. Spirals could not be done because the test fixture does not have enough clearance to allow for the top plane. The 2 oz experiments were omitted because the experimental results (Table 8-4) show a small difference between 1oz and 2 oz traces. The large circles and rectangles were deemed sufficient to demonstrate the dual plane techniques. Follow-on research considers the dual plane techniques in more detail.

The experiments were etched into 3 single sided 4x6 printed circuit board by a professional outfit (Figure 8-2). One board contains the circle experiments etched in 1oz (1.35 mils) copper. The other two boards contain identical rectangular and

spiral experiments; the difference between these two boards being only the thickness of the copper. One is etched in 1oz copper while the other is etched in 2oz (2.75 mils) cooper.


Figure 8-2: The Experimental Boards

To ensure accurate measurements and to reduce error cause by poor contacts, #6 brass screws were soldered to the pads (see Figure 8-3)
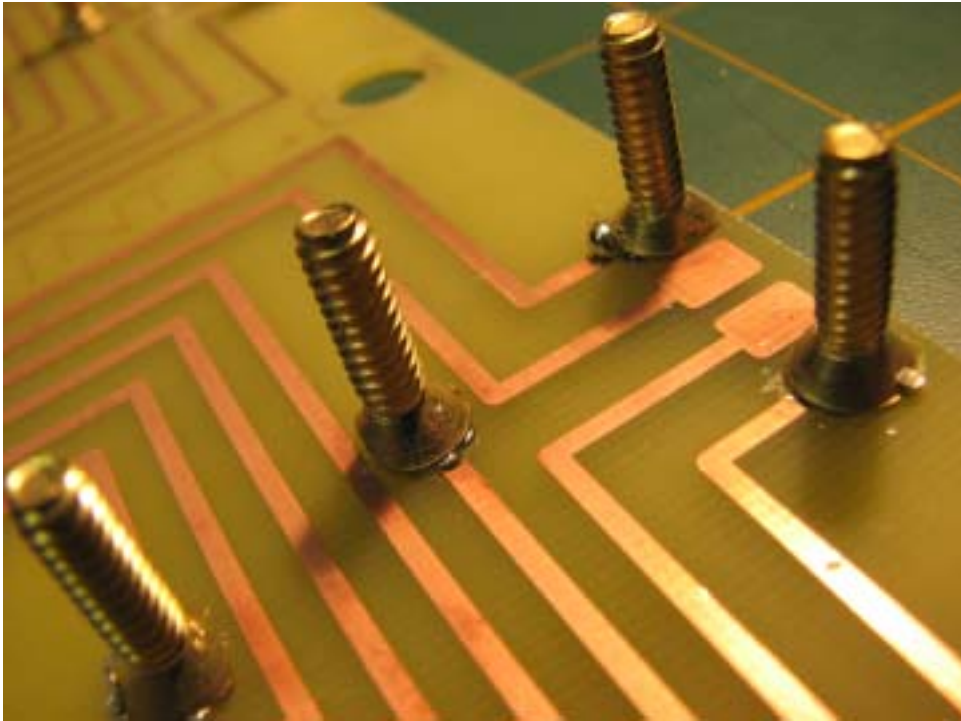
Figure 8-3: Brass Screws used as terminals

An Agilent E4980A Precision LCR meter was obtained to gather the experimental data (Figure 8-4). In order to ensure highly accurate and repeatable readings, a special fixture was developed (Figure 8-5) to couple the experiments to the meter. This fixture is compliant with the 4TP specification mentioned in the Agilent Technologies Impedance Measurement Handbook [IMPEDANCE] section 3-2.

The LCR meter was purchased new and still shows the yellow calibration traceability envelope attached.
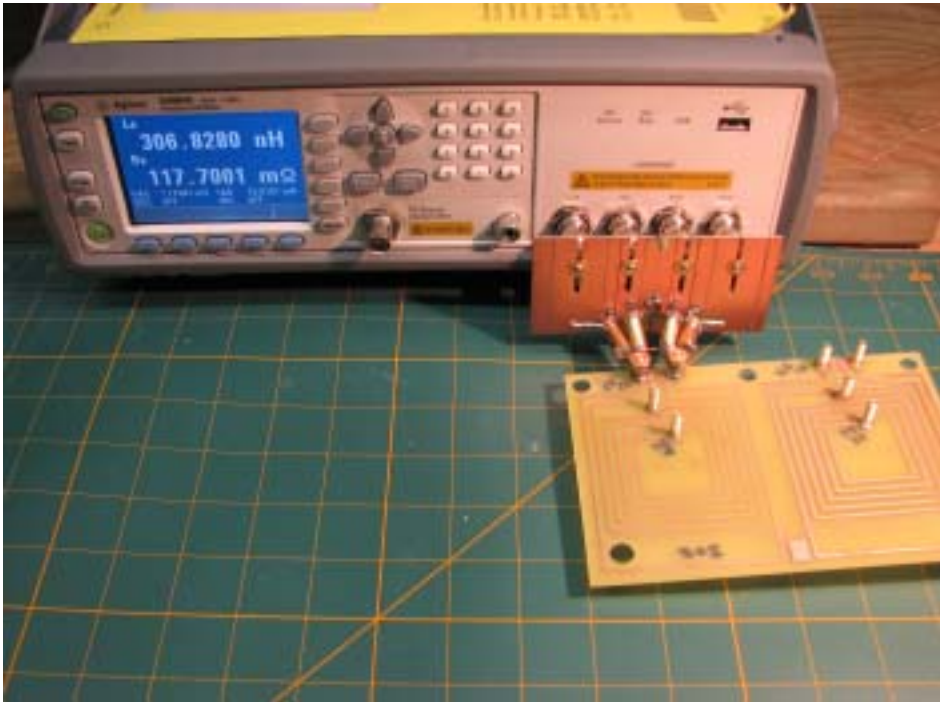
**Figure 8-4: Agilent E4980A Precision LCR meter**

¼ inch thick brass shorting block
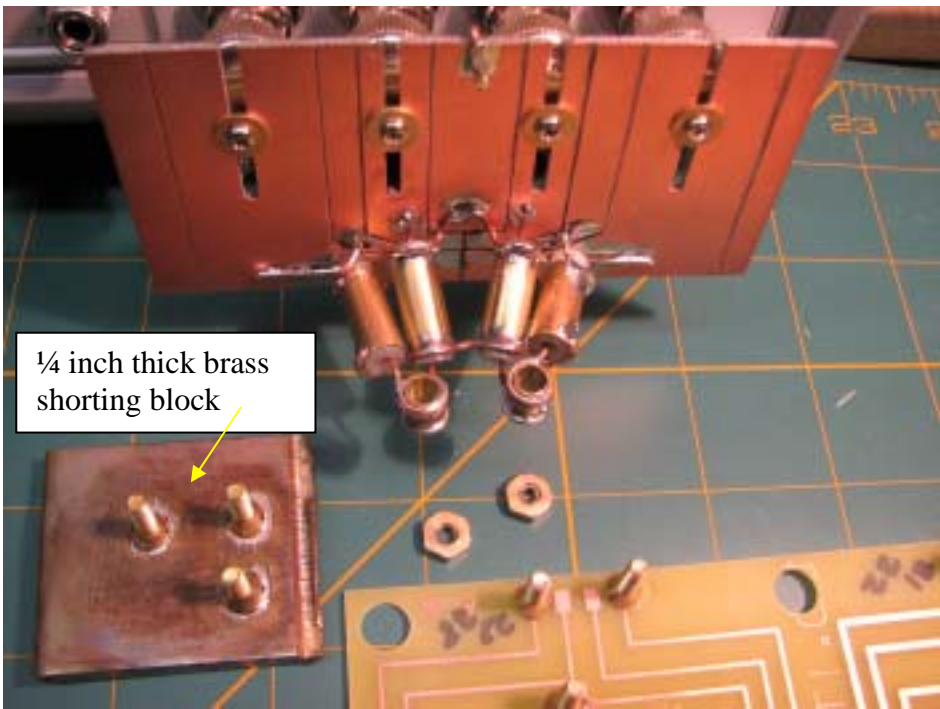
Figure 8-5: 4TP Test Fixture used for experiment

In order to compensate for impedance of the test fixture, the LCR meter provides for "Open" and "Short" compensation.

For "Open" compensation, the test fixture is left unconnected as shown in the following figure. In the "Open" compensation mode, the LCR meters measures the impedance of the test fixture at various frequencies and stores the information internally. Essentially, the "Open" compensation nullifies the parallel capacitance and leakage of the fixture from the measurements.

For "Short" compensation, a shorting block (shown in Figure 8-5) is attached to the fixture. The shorting block consists of a ¼ inch thick brass flat stock with terminal screws mounted similarly to the experiments. In the "Short" compensation mode, the LCR meter measures the impedance of the fixture at various frequencies and stores this information internally. Essentially, "Short" compensation nullifies the series inductance and resistance of the test fixture from the measurements.
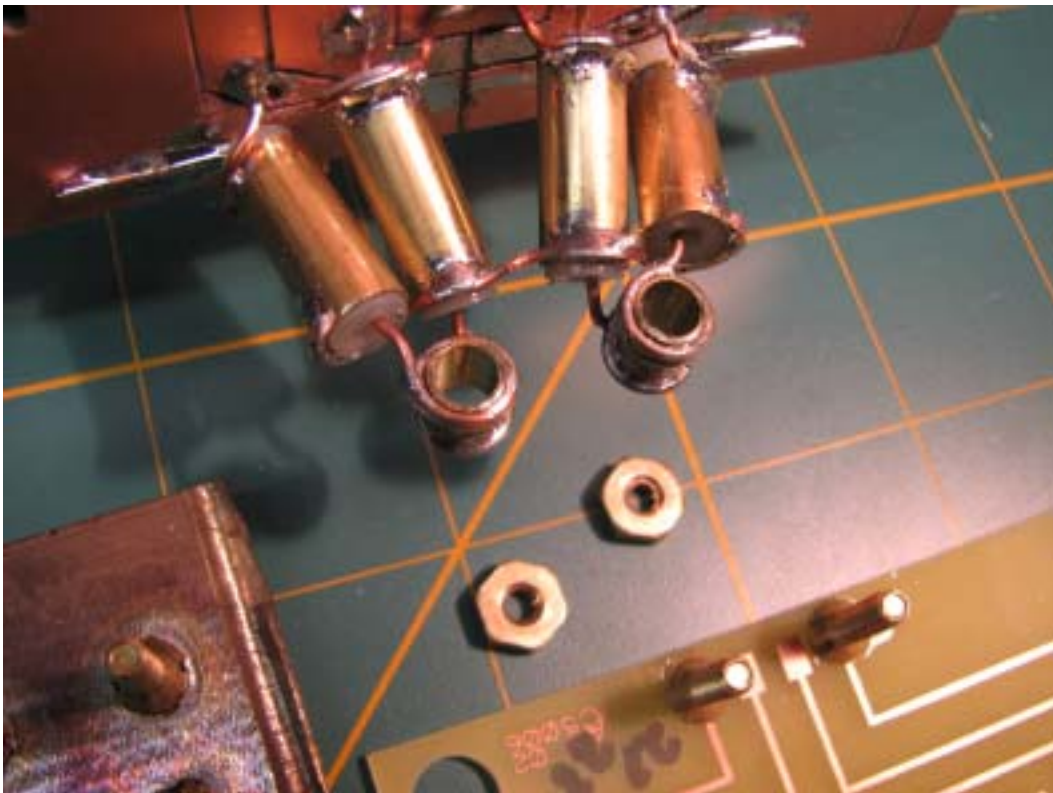

Figure 8-6: Close-up of Test Fixture

For experiments requiring a conducting plane (all of the even numbered experiments) an un-etched PCB is inserted under the inductor being measured (see Figure 8-7).
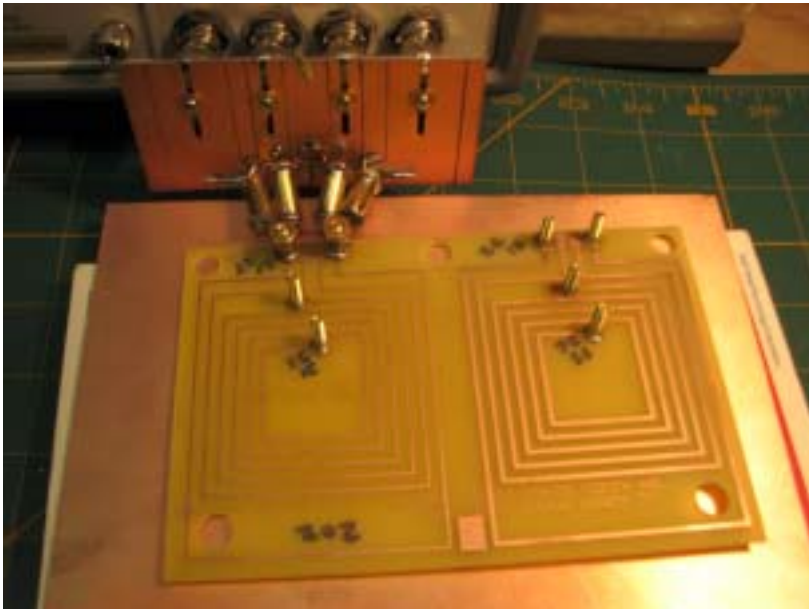

Figure 8-7: An un-etched 1oz PCB inserted underneath for measuring effects of single plane

In order to ensure that the inductor lays flat against the conducting plane, a "Keeper" was constructed from wood and hot-melt glue as shown in Figure 8-8. A thick text book was placed over the base of the keeper to ensure sufficient pressure (not shown).

For dual plane measurements, a second single-sided un-etched PCB is placed on top of the inductor being measured. It is oriented with the copper side up (see Figure 8-9).
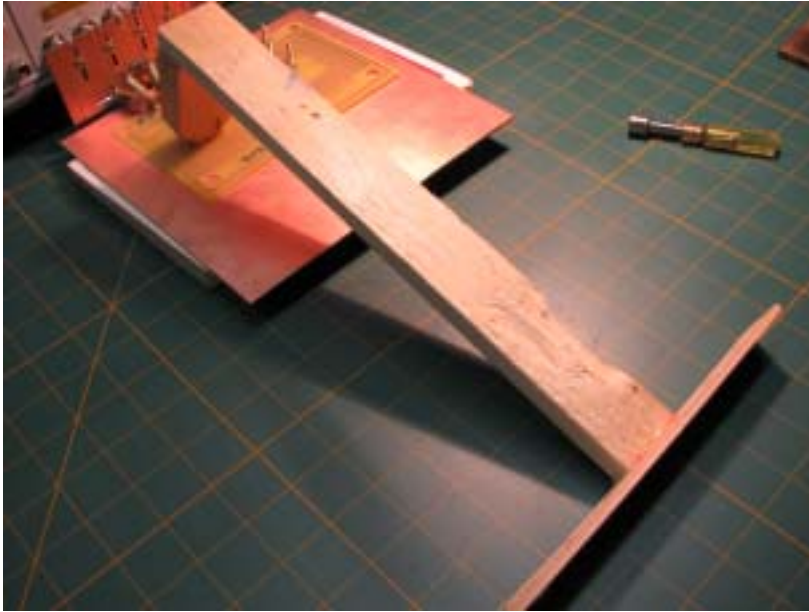
**Figure 8-8: The "wooden keeper" -- text books not shown**
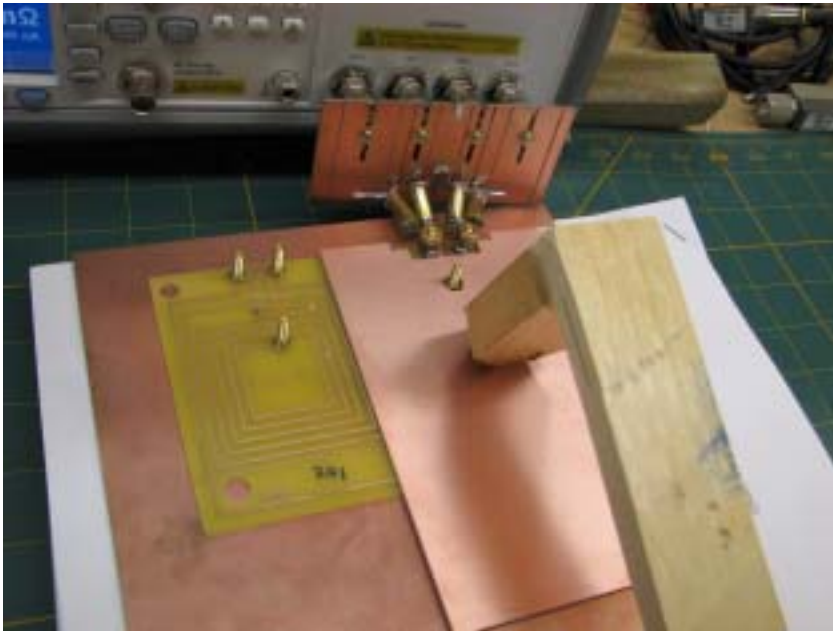
Figure 8-9: Dual Plane Measurement

8.1. Characterizing the LCR Meter and Fixture

This section highlights a procedure for evaluating the ability of the LCR meter to compensate for the Test Fixture.

This procedure begins by allowing the LCR meter to warm-up for 1 hour. Then both open and short compensations are performed. Following the compensation, the Shorting Block is installed and a set of 32 measurements, at different frequencies, are made. These measurements are plotted in Figure 8-10.

Since the LCR meter is not perfect there will be a residual inductance measured. At the higher frequencies, the residual error is only a few Pico Henries. The LCR meter was left running for 6 hours; after which, the same measurements were taken. The second set shows that the residual error grew by a factor of 10. At 2 MHz, the error was still less than 100 pH; therefore, as long as the measurements are taken within 2 hours of compensation, we can expect instrument drift no greater than 1 nH for frequencies 1 KHz and above.
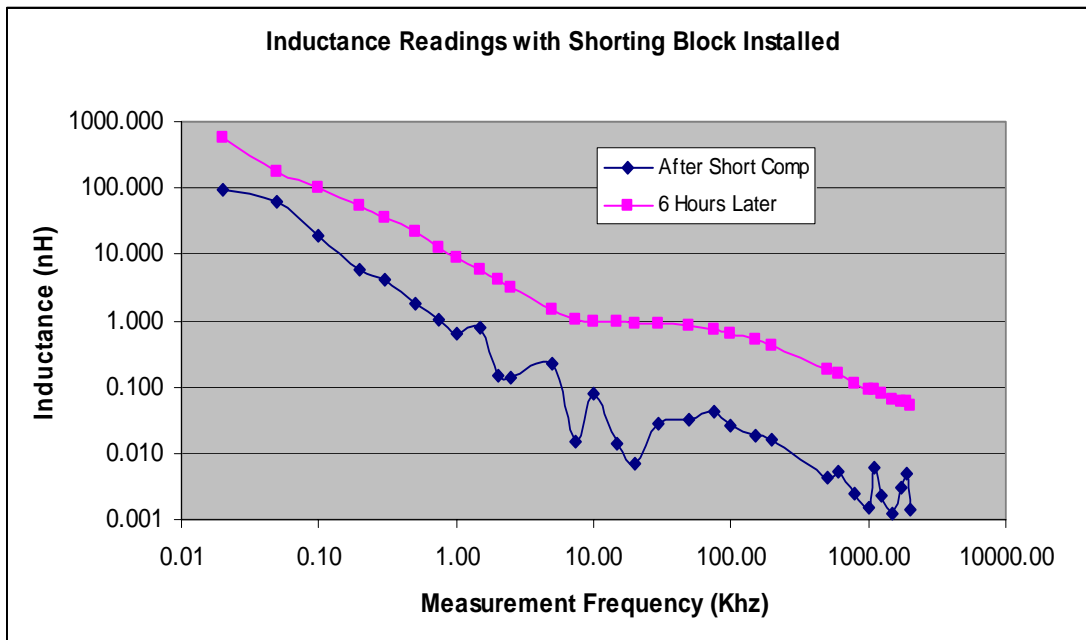
Figure 8-10: Compensation and compensation drift

8.2.   *Measurements*

It would be preferable to take all the measurements at a single frequency; however, due to frequency dependant errors (such as stray as capacitance) the value obtained from the LCR meter may not be the actual inductance.

To explore a measurement strategy, measurements are taken at 32 frequency points using the list mode of the LCR meter. The setup of the meter is shown in Table 8-3.

Table 8-3: LCR meter settings used for experiments

Frequencies	200,300,500,750,1K,1.5K,2K,2.5K,5K
	7.5K,10K,15K,20K,30K,50K,75K,100K,150K
Readings below 200hz are not reliable, for the inductors in this thesis.	200K,500K,600K,800K,1M,1.1M,1.25M
	1.5M,1.75M,1.9M,2M

Measurement Time (Aperture)	Long
Averages	32
Mode	Ls-Rs
Compensation	Open and Short – All measurements taken no later the 2 hours after compensation
All Other Settings	Default (power on)

Figure 8-11 plots the meter readings for experiments 11 and 12. The blue plot shows the reading of the experiment without the ground plane and the magenta plot is the reading with the ground plane. The yellow lines represent the computer predictions for the given experiments.

It is interesting to note that below 1 KHz, the plots for both experiments merge. This suggests that there is a certain M-field intensity required to knock electrons loose in the ground plane. Below this threshold, the ground plane does not affect the measurements.

After 100 KHz, both traces have an even downward slope which suggests that other stray effects are beginning to dominate.

What is needed is a logical criterion to pick a measured value from the LCR meter readings.
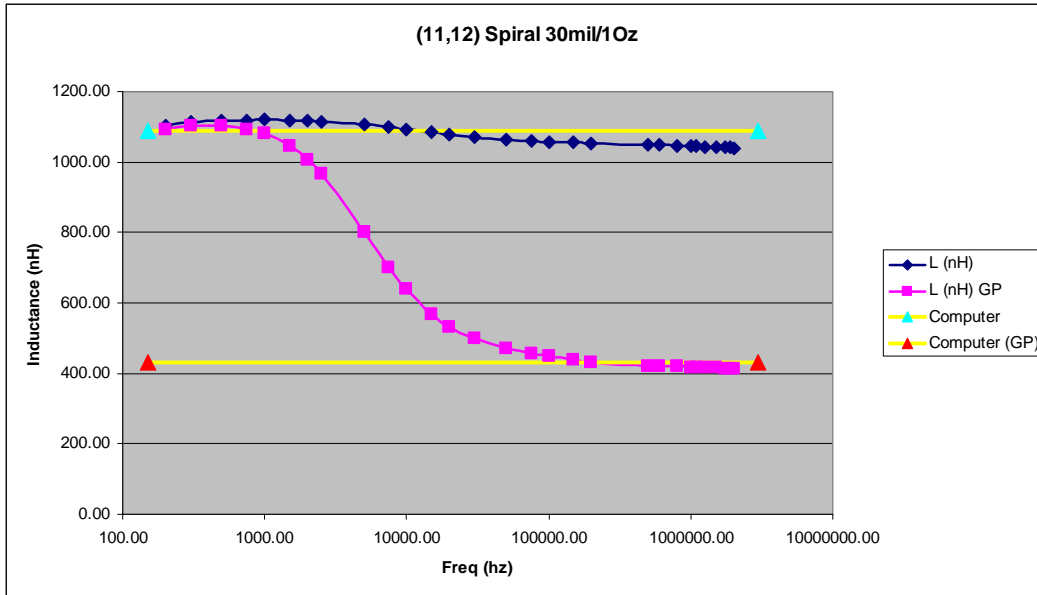
Figure 8-11: Measurement plot of experiments 11 and 12

Since the lower frequencies do not energize the conducting plane, then it is reasonable to conclude that other stray effects are minimal as well. Therefore, the measurements for experiments without conducting planes are to be declared where the blue and magenta traces intersect (or where they come closest to intersecting).

For the experiments with a ground plane, it would be preferable to choose the measurement point at the same frequency as the sans ground plane experiment. Since the ground plane is not energized at this point, we need to find a different method.

8.2.1.   LCR Correction Factor

Since the intersection of the plots in Figure 8-11 is the desired measurement for the sans ground plane experiments, then this knowledge is used to develop a correction factor.

We should like to take all measurements at 2 MHz since all ground plane effects are energized and there is minimal instrument drift. However, since other stray effects become more pronounced as frequency increases, then measurement error is to be expected. Therefore, a correction factor is needed to offset these other undesired effects (refer to Figure 8-12).

If the measurement at the intersection is what we define as the correct value for the non-ground plane experiment, and the measurement at 2 MHz for the non-ground plane experiment includes the correct value plus errors due to stray effects, then the stray effects are found by subtracting the two measurements.

Stray_Effects@2Mhz = Measurement@2Mhz – Measurement@Intersection

The negative of the stray effects is the correction factor.

CorrectionFactor@2Mhz = Measurement@Intersection - Measurement@2Mhz

This correction factor must be determined for each inductor. All measurements of this inductor made at 2MHz must be corrected by adding this factor. This includes single and dual plane measurements.
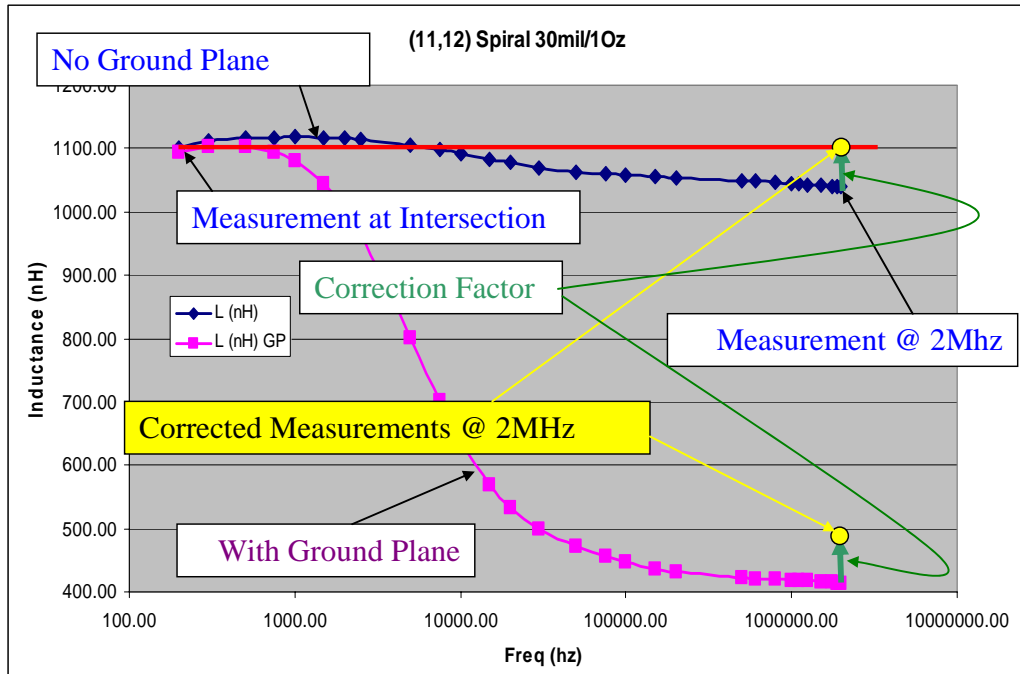
Figure 8-12: LCR measurement correction strategy

This correction factor is determined for each inductor shape being measured. The correction factor is then applied to all measurements of that inductor (with and without ground planes) to provide a measurement which is reasonably free of stray effects.

8.3. Experimental Data

Table 8-4 lists the computer prediction of a given experiment to the LCR meter readings for experiments without ground plane. The experiment numbers correspond to the experiment numbers found in Table 8-1.

Table 8-4: Experiments without Ground Plane

Exp #	Measured (nH)	Computed (nH)	%diff
1	274.0192	271.3814	1.0
3	223.9854	222.8745	0.5
5	1028.236	1029.098	-0.1
7	303.2772	299.5625	1.2
9	249.4881	247.4069	0.8
11	1101.615	1088.572	1.2
13	182.2881	176.6878	3.1
15	136.8191	133.4696	2.4
17	197.8299	195.2839	1.3
19	154.4495	149.1949	3.4
21	279.2265	269.9571	3.3
23	224.8992	221.6351	1.5
25	1034.499	1026.394	0.8
27	310.7126	297.2776	4.3
29	253.9133	245.4195	3.3
31	1110.758	1084.12	2.4

Figure 8-13 plots the computed value verses the measured values for each experiment in Table 8-4. The red line drawn through the chart represents the ideal line. If the measured value and computed value for a given experiment matched, then the plotted point will fall on the red line. Error in either measured or computed values will drive the experimental points farther from the red line. Figure 8-13 shows excellent agreement between computer and measured values.

Experiments w/o Ground Plane

$y = 0.9874x$

$R^2 = 0.9997$

Coefficient of Determination

Spirals

Average Abs Error =1.9%
Std Deviation of Error =1.3%

Single Turn Loops
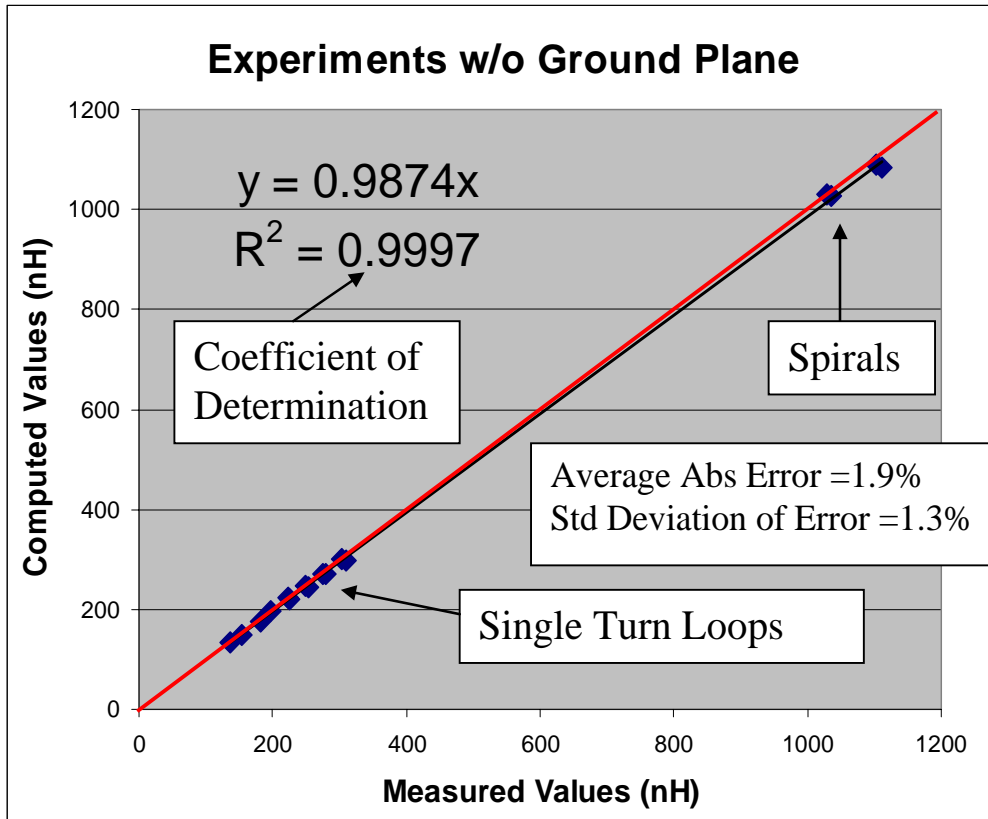
Figure 8-13

Table 8-5 lists the computer predictions and LCR meter readings for experiments with a ground plane. Figure 8-14 plots the computed value verses the measured values for each experiment in Table 8-5.

Table 8-5: Experiments with Ground Plane

Exp #	Measured (nH)	Computed (nH)	%diff
2	132.8018	141.1919	-6.3
4	117.0898	121.6218	-3.9
6	395.1197	371.9067	5.9
8	161.6237	169.2292	-4.7
10	142.992	146.0494	-2.1
12	475.773	431.0998	9.4

14	103.5605	94.09387	9.1
16	77.10436	76.95042	0.2
18	108.2925	112.4716	-3.9
20	94.19904	92.52247	1.8
22	139.2673	140.1886	-0.7
24	119.2943	120.7633	-1.2
26	398.2248	370.735	6.9
28	165.915	167.3749	-0.9
30	144.1099	144.4133	-0.2
32	470.8806	428.1903	9.1

Experiments W/Ground Plane

$y = 0.9393x$

$R^2 = 0.9922$

Average Abs Error $= 4.1\%$
Std Deviation of Error $= 3.3\%$
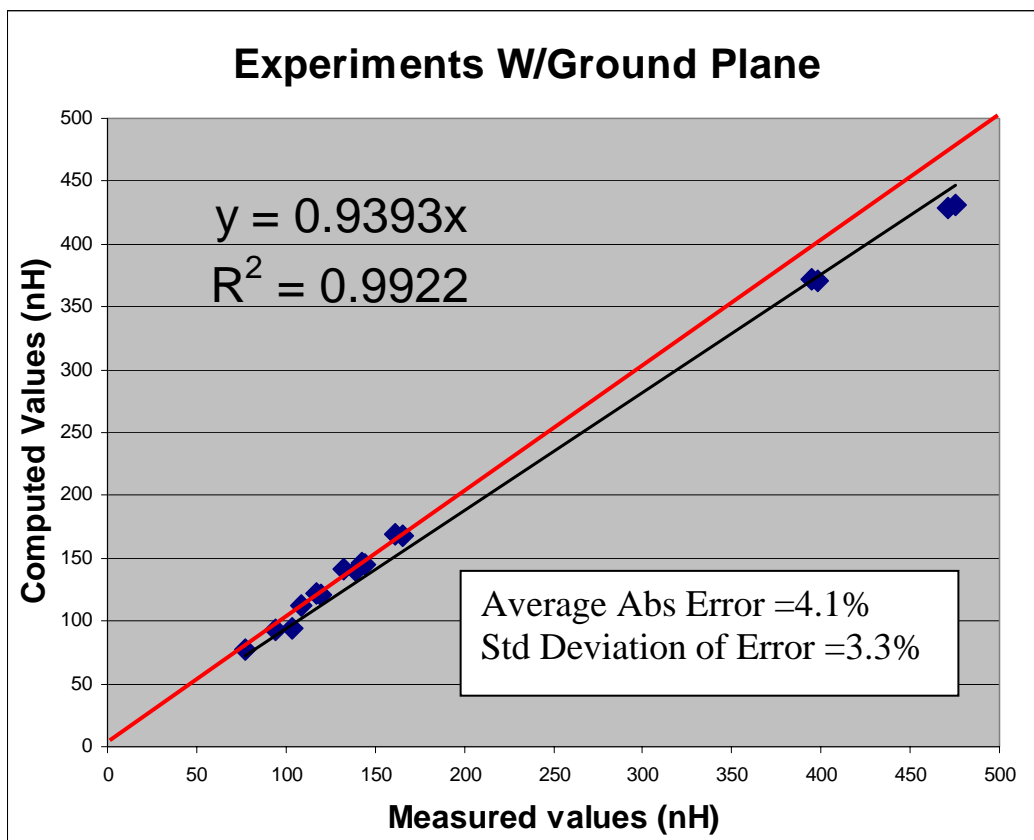
Figure 8-14

Figure 8-14 shows that the data taken with ground plane does not correlate as well as the non-ground plane experiments. This due to the following factors:

1) The addition of the ground plan increases parasitic capacitance which affects the measured result. This is more severe for the spirals since the

Page 75

traces have significantly more surface area. This makes the inductance
more difficult to measure accurately.

2) The ground plane reduces the overall inductance by more than 50%;
therefore, the measurements are closer to the instruments noise margin.

One must remember that the computer predictions are based on a uniform current
distribution (a simplification). Even with this simplification, accuracy is obtained
to within 5% for non-ground-plane experiments and 10% or better for
experiments with ground plane. These are certainly useful tolerance values since
inductor manufacturers, such as Toko, offer standard tolerances of 5% and 10%
[TOKO].

Table 8-6 contains the dual plane results and Figure 8-9 shows the data plotted.

Table 8-6: Dual Plane Experiments

| Exp #	Measured	Computed	%diff
33	112.2639	114.6488	-2.1
34	140.6	141.8519	-0.9
35	77.36	76.33011	1.3
36	92.67	94.26503	-1.7
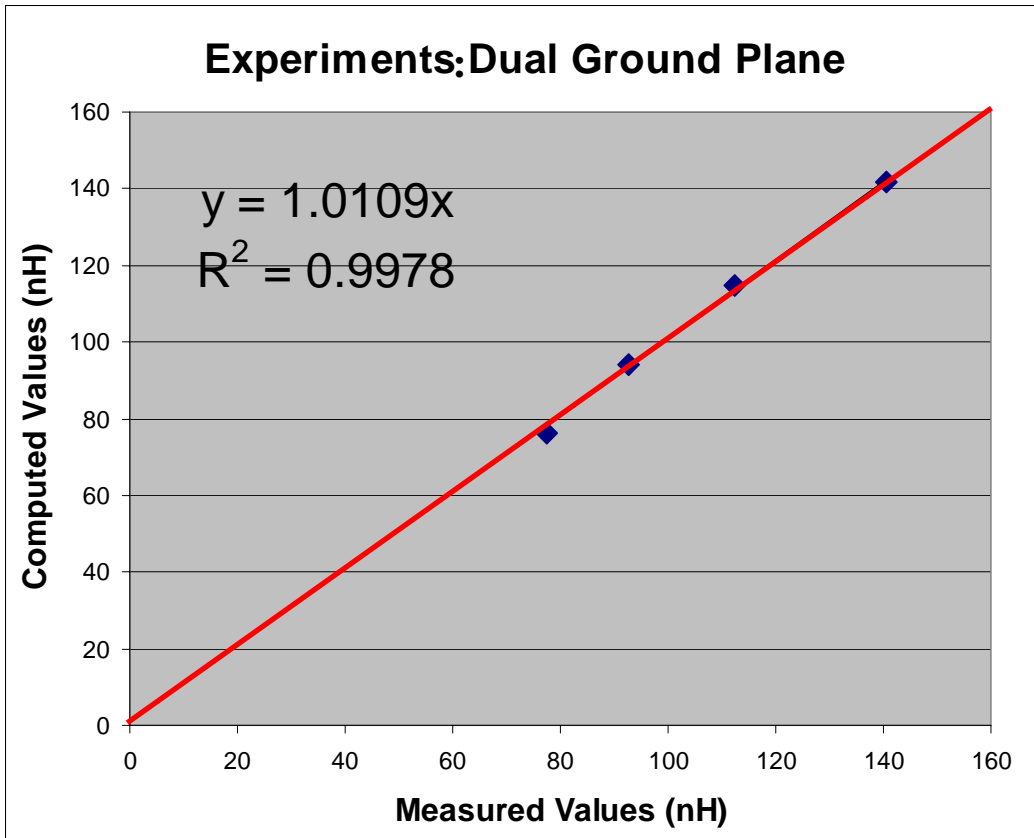
Figure 8-15: Dual Ground Plane Results

9.Processing Time Comparison

This section compares the processing time between the NE algorithm and the PI algorithm.

Only straight conductors of varying length are considered. This allows us to use PI without the need to break the conductor up into partitions.
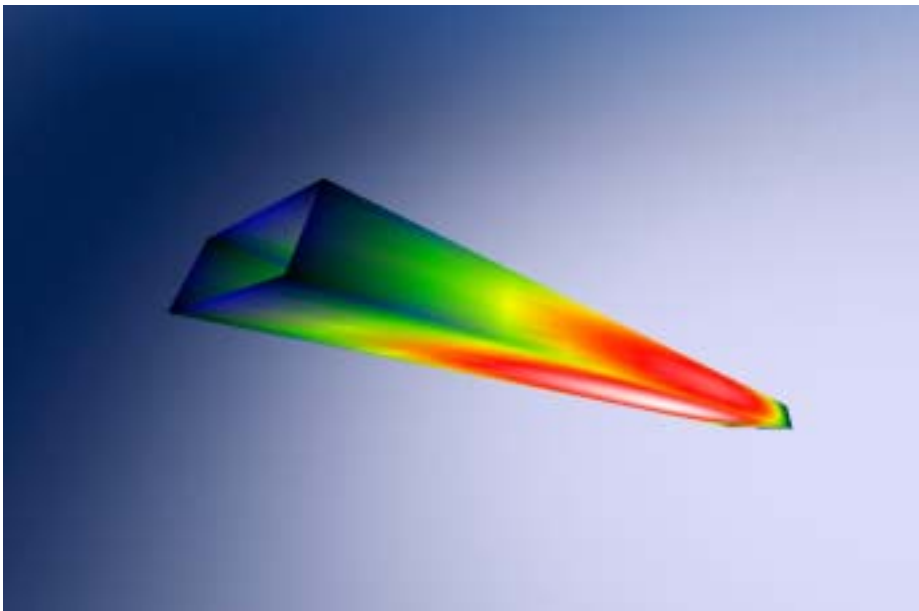

Figure 9-1: Straight Conductor

The conductors have a width of 30 mils and height of 2 mils. The length starts at 10 mils and continues to double until either process breaks a ½ hour time limit. The following chart compares the processing times.
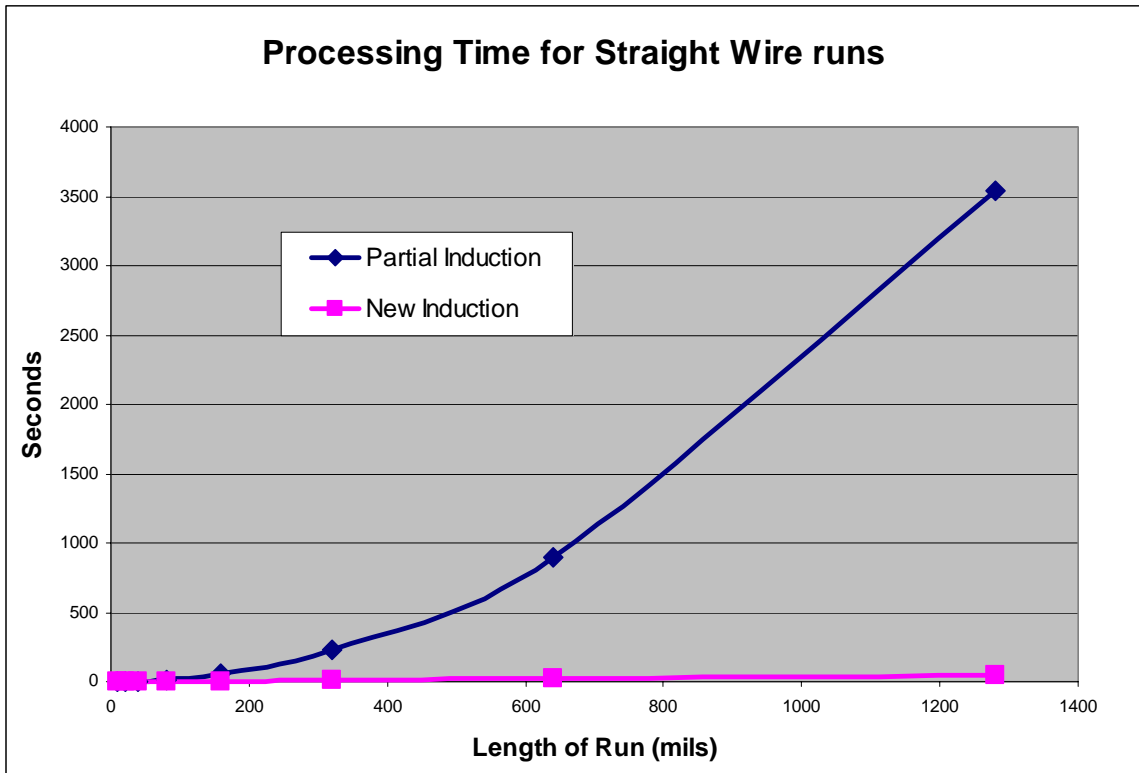
Figure 9-2: Processing Time Comparison

Since the height and width of the conductors are held constant, then the length is proportional to the volume of the conductor. This is important because both algorithms are volume integrals which mean that processing time is a function of volume.

The processing time for the NI algorithm is nearly linear with respect to wire volume. The processing time for PI increases by the square of wire volume. Therefore, the NI algorithm is nearly an order of magnitude faster than the PI algorithm.

There is further room for improvement in the NI algorithms. For example, expanding the seed size would reduce the integration time since more of the integration is pre-computed.

10.Conclusion

This thesis demonstrates the modeling of inductance using New Electromagnetism models and techniques. This is a preliminary work which simplifies the modeling by assuming that the current distribution in a conductor is uniform in cross section and along the length. This simplification is common to prior art reviewed; and gives reasonably good results for low frequency predictions as demonstrated by the excellent agreement between the theoretical and experimental results.

Also demonstrated is a simplified approach to modeling ground plane effects for both single plane and dual plane cases. This technique employs a negative image of the circuit trace current. The image appears once for a single plane implementation and multiple times for the dual plane implementation. This is a more complete and simpler approach than the PI method [Holloway] which only considers the single plane case in a return path configuration. The NE approach produces results which are consistent with experiment.

This thesis further shows that all valid derivations of inductance based on CE are singular. Those derivations that are not singular are shown to be erroneous. PI is the industry standard model; ironically, it is both singular and in violation of CE.

The NE approach provides for numerical integration algorithms that are at least an order of magnitude faster than PI. Furthermore, since the NE approach is not singular, it is therefore inherently stable.

The next phase in this research involves the modeling of non-uniform charge motion in a conductor. This will require the use of all New Electromagnetism models to provide predictions of circuit properties which include capacitance,

inductance, skin-effect and others. One of the goals being the ability to model a circuit geometry with enough precision and detail to predict the LCR meter readings at any frequency and mode. The ultimate goal being broad spectrum modeling of circuit dynamics to include transmission line modeling and antenna performance.

11.References

[FCC] The following internet sources were used for the section on copper structure http://www.ndt-ed.org/EducationResources/CommunityCollege/Materials/Structure/metallic_structures.htm and
http://www.science.uwaterloo.ca/~cchieh/cact/applychem/metals.html

[Hayt] Hayt, William H., 1981. Engineering Electromagnetics, Fourth Edition. McGraw-Hill Inc., New York.

[Holloway] Holloway, Christopher L. et al., 1998. Net and Partial Inductance of a Microstrip Ground Plane, IEEE transactions on electromagnetic compatibility, Vol. 40, No. 1.

[IMPEDANCE] (no Author listed), Agilent Impendence measurement hand book. July 2006 http://cp.literature.agilent.com/litweb/pdf/5950-3000.pdf

[ind_jackson] Distinti, Robert J., 2004. A classical Attempt at Induction, www.distinti.com/docs/ind_jackson.pdf.

[Jackson] Jackson, John David, 1999. *Classical Electrodynamics*, Third Edition. John Wiley and Sons Inc., Hoboken, NJ. On page 181 is found a solution to a current ring using Vector Magnetic Potentials.

[LCR1] (no author), November 2006. Agilent E4980A LCR meter users manual. Third Edition. http://cp.literature.agilent.com/litweb/pdf/E4980-90020.pdf

[Lorraine] Lorrain, Paul, 1988. Electromagnetic Fields and waves, Fourth Edition. W.H. Freeman and Company, New York.

[Maxwell] Maxwell, James Clerk, 1891. A Treatise on Electricity And Magnetism, Unabridged Third Edition, Dover. New York. This is a two volume set first printed by Dover in 1954.

[NE_intro] Distinti, Robert J., 2005. New Electromagnetism Introduction. www.distinti.com/docs/ne_intro.pdf

[NI] Distinti, Robert J., 1997. New Induction, www.distinti.com/docs/ni.pdf

[NI_neumann] Distinti, Robert J., 2003. New Induction and the Neumann Equation, www.distinti.com/docs/ni_neumann.pdf

[NM] Distinti, Robert J., 2001. New Magnetism, Area-46 Publishing, Fairfield, CT. www.distinti.com/docs/bk_000.pdf.

[Pozar] Pozar, David M., 2005. Microwave Engineering, Third Edition. John Wiley & Sons, Inc. Hoboken, New Jersey.

[Ruehli] A. E. Ruehli, *Inductance Calculations in a Complex Integrated Circuit Environment*, IBM Thomas J. Watson Research Center, Yorktown Heights, New York.

[Secrets] Distinti, Robert J., 2004. The Secrets of QvxB, www.distinti.com/docs/the_secrets_of_qvxb.pdf

[TOKO] (no author), Toko wire wound chip inductor catalog. http://www.toko.co.jp/products/pdf/inductors/llm3225.pdf

[Weber] Weber, E., 1965. Electromagnetic Theory, Dover, New York.

Appendix A: Material Constants

Material	Charge Mobility $\mu_e \left[\dfrac{m^2}{Vs} \right]$	Conductivity $\sigma \left[\dfrac{1}{\Omega m} \right]$	*Charge Density* $\rho = \dfrac{\sigma}{\mu_e} \left[\dfrac{Q}{m^3} \right]$
Copper	0.0032	$5.80\text{x}10^7$	*$1.8125\text{x}10^{10}$*
Aluminum	0.0012	$3.82\text{x}10^7$	*$3.1833\text{x}10^{10}$*
Silver	*0.0056*	*$6.17\text{x}10^7$*	*$1.102\text{x}10^{10}$*

Appendix B: Glossary

1oz	Thickness of copper equal to 1.35 mils
2oz	Thickness of copper equal to 2.75 mils
4TP	Four Terminal Pair lead configuration. It is the best method according to the Agilent Impedance Measuring Handbook.
A	Cross sectional Area of conductor.
B	Magnetic field intensity in Webbers per square meter. (classical theory only)
CE	Classical Electromagnetic field theory.
emf	Electro motive force.

FCC	Face Center Cubic. This is the manner in which copper atoms arrange themselves in metallic copper. In fact most conductors have this arrangement.
H	The Height of the copper trace.
I	Current in Amperes.
IC	Integrated Circuit
J	Current Density in Amperes per unit area.
KE	Kinetic Energy
K_E	Electric field Constant $$K_E = \frac{1}{4\pi\varepsilon}$$
K_M	Magnetic field Constant $$K_M = \frac{\mu}{4\pi}$$
L	L = inductance **L** = vector unit of length
LCR	Inductance Capacitance Resistance
M	M = mutual inductance **M** = vector M-Field
mil	A unit of length equaling 0.001 inches
N	Total number of FCC cells in a seed
NE	New Electromagnetism
NI	New Induction
NM	New Magnetism
Ns	Number of FCC cells on the side of the seed

P	The number of moving charges per copper atom (typically a fractional number)
PCB	Printed Circuit Board
PE	Potential Energy
PI	Partial Inductance Model
Q	A quantity of charge in coulombs
RLC	Resistance Inductance Capacitance
RSV	Raw Seed Value
S	The length of one side of the seed
Seed	A small section of a conductor where the inductive effects are computed at the atomic level.
Source Charge	The charge that is creating the field that is being studied
Target Charge	The charge that is reacting to the field that is being studied
VMP	Vector Magnetic Potentials
W	Width of a PCB or IC trace

1